# Analyses of the Regulation of Coccolith Production by Environmental Factors and a Protein Associated with Coccolith Production by a Coccolithophorid, *Emiliania huxleyi*

November 2008

Manami SATOH

# Analyses of the Regulation of Coccolith Production by Environmental Factors and a Protein Associated with Coccolith Production by a Coccolithophorid, *Emiliania huxleyi*

A Dissertation Submitted to
the Graduate School of Life and Environmental Sciences,
the University of Tsukuba
in Partial Fulfillment of the Requirements
for the Degree of Doctor of Philosophy in Science

Manami SATOH

Table of Contents

Abbreviations

AP: alkaline phosphatase

ATPase: adenosine triphosphatase

BiP: immunoglobulin heavy-chain-binding protein

CAPS: 3-(cyclohexylamino)-1-propane sulfonic acid

CyP: cyclophilin

Da: dalton

DIC: dissolved inorganic carbon

ER: endoplasmic reticulum

ESM: Erd-Schreiber's medium

EST: expression-sequence-tag

FKBP: FK506-binding protein

MA: Marine Art SF

PAGE: polyacrylamide gel electrophoresis

Pi: inorganic phosphate

PPIase: peptidyl-prolyl *cis-trans* isomerase

SDS: sodium dodecyl sulfate

Tris: tris (hydroxymethyl) aminomethane

Abstract

A marine unicellular alga, the Coccolithophorid, *Emiliania huxleyi* produces scales mainly consisting of calcite ($CaCO_3$) crystals, that are called coccoliths. The coccoliths are produced intracellularly by biomineralization, transferred to outside of the cell and placed on it. Many molecules are seemed to be involved in the process, but knowledge on such molecules, especially protein factors, have not been identified.

In this study, I firstly attempted to elucidate a physiological regulatory mechanism of coccolith production by environmental factors and period when coccolith production was stimulated. Based on the results, I intended to elucidate a molecular mechanism of coccolith production by identifying a protein associated with the coccolith production and finally characterized the protein synthesized *de novo* during active coccolith production.

In order to stimulate coccolith production, cells were placed under both phosphate-deficient and low temperature conditions. In a batch culture, orthophosphate in the medium (final concentration, 28.7 μM) was rapidly depleted. Under such conditions, extracellular alkaline phosphatase (AP) activity, an indicator of phosphate deprivation, increased during the stationary growth phase. The increase in AP activity was slightly higher at 20°C than at 12°C. The calcification started to increase earlier than AP activity and the increasing rate was much higher at 12°C than at 20°C. Such enhancement of calcification was suppressed by the addition of phosphate while AP activity was also suppressed after a transient increase. These results suggest that phosphate deprivation is a trigger for calcification and that a rather long induction period is needed for calcification compared to the increase in AP activity. While

calcification was greatly stimulated by cold stress, cellular activities such as growth, phosphate utilization and the induction of AP activity were slightly suppressed. The stimulation of coccolith production by cold stress was minimal under phosphate-sufficient conditions. The high calcification activity estimated by $^{45}Ca$ incorporation was confirmed by morphological observations of coccoliths on the cell surface under bright-field and polarization microscopes. These results indicate that phosphate deprivation is the primary factor for stimulating coccolith production, and cold stress is the secondary acceleration factor that stimulates calcification under conditions of phosphate deprivation.

In order to identify proteins involved in intracellular calcification by *E. huxleyi*. Proteins synthesized *de novo* under coccolith-production stimulating conditions were searched. For the analysis, the profiles of protein bands on SDS-PAGE were compared between cells grown:

1) under phosphate-deficient and phosphate-sufficient conditions.

2) under phosphate-deficient and phosphate-refeeding conditions.

3) at different temperatures, namely 20°C and 12°C.

In these experiments, I found a protein synthesized specifically when coccolith production was stimulated and then purified the protein. On 2D-SDS-PAGE, the apparent molecular mass and the isoelectric point (pI) of the protein were 32-kDa and approximately 4.2, respectively. From the determination of its N-terminal amino acid sequence by Edman degradation method, its deduced amino acid sequence was determined and then the sequence was brought to homology search in both expressed-sequence-tag (EST) and genome database of *E. huxleyi*. I found that the sequence of the protein shows a homology with a highly conserved FK506-binding

protein (FKBP) domain with the calculated molecular mass of 21,767. I named the protein EhFKBP21. FKBP is one of peptidyl-prolyl *cis-trans* isomerases (PPIase) which catalyse the interconversion of the *cis* and *trans* isomers of the peptidyl-prolyl (Xaa-Pro) bonds in peptide and protein substrates. The first 14 residues of the deduced amino acid sequence were predicted to be the signal peptide and EhFKBP21 contained an endoplasmic reticulum (ER) retention sequence KDEL at the C-terminal, suggesting the localization in ER. Some FKBPs localized in ER have been reported to associate with one or more proteins and expected to be involved in quality control system. The sequence also contains two calcium binding motifs (EF-hand motifs) at C-terminal side of FKBP conserved domain. In literature, two functions of EF-hand were reported, namely the one is $Ca^{2+}$-buffering and the other is $Ca^{2+}$-depending regulation. Therefore, the protein EhFKBP21 was predicted to be regulated by calcium concentration in ER.

In this study, I found that phosphate deprivation is the primary factor for stimulating coccolith production, and cold stress is the secondary factor to enhance the calcification under Pi-limiting condition. I also found a protein synthesized *de novo* when coccolith production was stimulated. I named the protein EhFKBP21 based on its deduced molecular mass and a FKBP-type PPIase domain. It is expected that the protein is located in ER and its activity is regulated by calcium. However, its detailed function and relationship with coccolith production remained to be elucidated.

## General Introduction

Biomineralization refers to the processes of mineral formation by organisms and the minerals formed are called as biominerals. Biomineralization is widespread in the biological world, namely bacteria, protists, plants and animals. Among over 60 kinds of known biominerals, one of the most abundant is calcium carbonate (Baeuerlein, 2000). The minerals formed by biologically-regulated biomineralization have unique crystal structures which are different from those produced by inorganic mineral formation, thus the mechanism of biologically-regulated biomineralization gains much attention in not only biology but also material engineering.

Coccolithophorids, marine unicellular algae classified in the division Haptophyta, produce huge blooms in the ocean especially at high latitude. Moreover, they have gained a great deal of attention as important players in charge of the global climate and the carbon cycle. These algae are capable of fixing carbon by both photosynthesis to produce organic matter and calcification to produce $CaCO_3$ crystals. Calcified shells of coccospheres consist of calcareous blocks with complex shapes and are called coccoliths. Shape of coccolith differs according to species or phase. *E. huxleyi* is the most cosmopolitan coccolithophore species and is used for numerous comparative physiological studies as it grows well in laboratory culture (Winter et al., 1994; Paasche, 2002).

The amount of coccolith production by *E. huxleyi* is affected by various environmental conditions (Zondervan, 2007). Lower salinity suppresses coccolith production (Paasche et al., 1996; Green et al., 1998), and especially low calcium concentration inhibits the calcification even when cellular photosynthetic activity is kept

unchanged (Paasche, 1964; Trimborn et al., 2007). Enrichment with $HCO_3^-$ increases coccolith production (Takano et al., 1995). As calcium and $HCO_3^-$ are substrates for coccolith production, these changes can easily be predicted. Either nitrogen deprivation or phosphate deprivation stimulates coccolith production (Paasche and Brubak, 1994; Paasche, 1998), but the mechanisms for the stimulations are still unknown. Cold stress was also reported to stimulate coccolith production (Sorrosa et al., 2005).

Molecular mechanism of coccolith production and its morphological control of crystals have been interested in various fields of science and technology, and the elucidation of mechanism is progressing. From the coccolith of *E. huxleyi*, an acidic polysaccharide was isolated and analyzed and expected to be involved in the regulation of coccolith crystal formation (Fichtinger-Schepman et al., 1979; Fichtinger-Schepman et al., 1980; Fichtinger-Schepman et al., 1981). It is also reported that coccoliths of other coccolithophorids, *Pleurochrysis carterae* and *Pleurochrysis haptonemofera* also contain 4 and 3 polysaccharides, respectively (Marsh et al., 1992; Ozaki et al., 2001; Hirokawa et al., 2005). There is a few report on molecules which likely to associate directly with coccolith production. One of them is GPA, a $Ca^{2+}$-binding protein which is isolated from intracellular polysaccharide fraction of *E. huxleyi* (Corstjens et al., 1998). The other is a V-type ATPase which isolated from coccolith vesicle in *P. carterae* and the protein is expressed constitutively (Araki and González, 1998; Corstjens et al., 2001; Corstjens and González, 2004). Recently, molecular biological approaches have been used for screening of molecules which associate with coccolith production (Quinn et al., 2006; Fujiwara et al., 2007). However, more than a half of the candidate proteins have no homolog description and therefore the knowledge on such proteins associated with coccolith production is necessary for further study on molecular mechanism of the

biologically-regulated calcification.

In this thesis, I attempted to elucidate regulatory and molecular mechanisms of coccolith production. Firstly, I proved that phosphate deprivation is the primary regulation factor for inducing coccolith production even under low temperature condition. Secondly, based on the results, I addressed identification and characterization of a protein synthesized *de novo* during the stimulation of coccolith production, expecting that the protein is associated with coccolith production directly or indirectly.

# Chapter I

Analyses of the Regulation of Coccolith Production by Environmental Factors in *Emiliania huxleyi*

Summary

Calcification of the Coccolithophorid, *Emiliania huxleyi*, is stimulated by many environmental factors like phosphate deficiency and low temperature. I examined effect of cold stress on calcification in combination with phosphate availability to elucidate the relationship between those factors. Inorganic phosphate (Pi) in the medium was exhausted in 3 days irrespective of the culture temperatures at 20°C as a control and 12°C as a cold stress, and then AP activity increased during the stationary growth phase. Calcification activity was much higher at 12°C than at 20°C although the change in alkaline phosphatase (AP) activity showed an opposite trend. The enhancement of calcification was almost negated by addition of Pi. Morphological features of coccolith production were investigated by using microscope and showed the same result with $^{45}$Ca-incorporation experiments on calcification. These results indicate that calcification is greatly enhanced by cold stress under phosphate deficient conditions and greatly repressed by the presence of sufficient phosphate.

## Introduction

Under natural conditions in the ocean, *E. huxleyi* is the most temperature-tolerant coccolithophore species (1–30°C) (Okada and McIntyre, 1979). Such tolerance to wide temperature range is from data of various species that have different temperature-dependence because of different environmental conditions of isolation sites. Those various species were isolated from different waters. In the laboratory, the maximum growth rate of *E. huxleyi* isolated in the Great Barrier Reef occurs at 25°C and no growth was observed at 10°C. The sizes of protoplasts and coccospheres increase when the growth temperature decreases. Quantitative analysis revealed that coccolith production was enhanced after a lag period when the cells were transferred from 20°C to 10°C in batch culture (Sorrosa et al., 2005).

Low temperatures also stimulate the degree of saturation and the amount of alkenones ($C_{37}$–$C_{39}$ long-chain ketones) in *E. huxleyi*. A number of unsaturated bonds in the molecules change depending on the growth temperature. Thus, the degree of $C_{37}$ alkenone saturation has been used as an assessment of palaeotemperature in organic geochemistry (Brassell et al., 1986; Prahl and Wakeham, 1987). Whether or how alkenone production is related to coccolith production, however, is still unknown, although both processes are stimulated at low temperatures.

Coccolith production is also regulated by other environmental factors. It is significantly enhanced by acute phosphorous shortage accompanied by growth cessation, and the ratio of carbon deposited in coccoliths to carbon converted to organic matters by photosynthesis (C/P ratio) is increased by phosphate deficiency. Moreover, coccolith production ceased immediately upon the re-addition of phosphate (Paasche, 1998).

Phosphate limitation also triggers an increase in AP activity, which is recognized as an indicator of phosphate deficiency in phytoplankton (Perry, 1972; Dyhrman and Palenik, 1999; Hoppe, 2003). *E. huxleyi* possesses two APs, one of which is constitutive and the other inducible by phosphate deficiency (Riegman et al., 2000). The latter was localized to the cell surface and it demonstrated no significant similarity to previously sequenced APs (Dyhrman and Palenik, 2003; Xu et al., 2006).

In this chapter, I investigated how cell growth, extracellular AP activity, and coccolith production, as estimated by $^{45}Ca$ incorporation, are associated with changes in temperature and phosphate availability in *E. huxleyi*. This information is important for our understanding of the relationship between phosphate availability and temperature to oceanic carbon flux and useful for determination of the conditions which coccolith production is enhanced.

Materials and Methods

## Organism and Culture Conditions

The coccolithophorid, *E. huxleyi* (Lohman) Hay & Mohler (NIES 837), Haptophyceae, was grown in artificial seawater (Marine Art SF; produced by Tomita Seiyaku Co., Ltd., Tokushima, formerly distributed by Senju Pharmaceutical Co., Osaka, Japan, and recently by Osaka Yakken Co. Ltd., Osaka) enriched with Erd–Schreiber's medium containing 10 nM sodium selenate instead of soil extracts (MA-ESM) (Danbara and Shiraiwa, 1999). Cells were maintained under constant illumination at 100 $\mu mol \cdot m^{-2} \cdot s^{-1}$ and 20°C (standard condition). Cells in early linear growth phase were transferred to 12° or 13°C for low temperature treatments. For Pi-deficient condition, cells in early linear growth phase were collected by weak centrifugation (550 × *g*, 10 min), washed with phosphate-free MA-ESM, resuspended in the fresh one.

## Measurement of Inorganic Phosphate Concentration in Culture Medium

The inorganic phosphate concentration in the medium was assessed by the molybdenum blue method (Murphy and Riley, 1962). Cells were removed from an aliquot of the culture medium by filtration before assessment.

## Determination of Alkaline Phosphatase Activity

AP activity was measured according to Reichardt et al. (1967) using *p*-nitrophenyl phosphate (*p*-NPP) as a substrate. Then 100 µL of 36 mM *p*-NPP and 700 µL of 200 mM 3-(cyclohexylamino)-1-propane sulfonic acid (CAPS) buffer at pH 10.0 were added to 200 µL of the cell suspension and incubated at 40°C for 15 min. The

reaction was terminated by the addition of 100 μL 4 M NaOH. The absorbance at 397 nm was measured using a UV-VIS spectrophotometer (UV mini 1240; Shimadzu, Kyoto, Japan).

### $^{45}$Ca Tracer Experiments for Calcification

First, 4.2 kBq/mL of $^{45}CaCl_2$ (18~28 GBq/mmol, Perkin-Elmer, Waltham, MA or 48 GBq/mmol, GE Healthcare UK Ltd, England) was injected to initiate the $^{45}$Ca-labeling reaction. At appropriate intervals 400 μL of culture was harvested and the cells were collected by centrifugation (10,000 × *g*, 5 min). The pellet was washed with fresh medium and transferred to a scintillation vial containing 0.5 mL of scintillation cocktail, Hionic-Fluor (Perkin-Elmer). The radioactivity incorporated into the coccosphere and the cytosolic space together was determined. Then the cells were harvested by filtration using an Ultrafree-MC filter (pore size, 0.65 μm; Millipore, Billerica, MA). The coccosphere was removed by washing in medium adjusted to pH 3.0 with HCl. Naked cells obtained on the filter were washed twice with the acidic medium and the radioactivity determined using a liquid scintillation counter (LS 5000TD; Beckman, Fullerton, CA). Radioactivity contained in the naked cells was treated as incorporated $^{45}$Ca in cytosolic space.

### Microscopic Observation

Cell number was determined by counting under a microscope (BX50; Olympus, Tokyo, Japan). Coccoliths surrounding the cells were observed with polarized light, and micrographs were taken using a microscope (DMR; Leica, Wetzlar Germany) equipped with a fluorescence microscope digital camera (Keyence, Osaka, Japan).

Results

### $^{45}$Ca-Incorporation into the Coccoliths and Cells of *E. huxleyi*

Figure I-1 shows that $^{45}$Ca incorporated into *E. huxleyi* cells was primarily distributed to the coccospheres. During the initial 10 h of growth, less than 90% was incorporated into coccospheres, and then the amount gradually increased to over 97% for the following 2 d (Fig. I-1). The results demonstrated that the amount of $^{45}$Ca incorporated by whole cells can be considered as that used for calcification including coccolith production.

### Effects of Phosphate Concentration and Cold Stress on Calcification by *E. huxleyi*

Growth of *E. huxleyi* was suppressed when the temperature was suddenly lowered from 20° to 12°C during logarithmic phase growth. The cells reached stationary phase following an initial 2 d lag in growth (Fig. I-2).

Orthophosphate added to the medium (final concentration, 28.7 μM) was depleted in the batch culture during 2.5 d at 20°C, although the rate of Pi depletion and time needed for Pi-depletion changed depending on pre-culture conditions and initial cell density. The decrease in temperature to 12°C suppressed growth transiently and caused delay of $P_i$ depletion. Extracellular AP, known to be synthesized *de novo* under $P_i$ deprivation (Xu et al., 2006), began to increase 4 d after the initiation of culture, irrespective of temperature change. It took 1–2 d to initiate AP induction after $P_i$ was removed from the medium. The increase in AP activity was less at 12°C than that at 20°C, although the difference was small, suggesting that the timing of the enzyme induction is mainly regulated by $P_i$ availability in the medium and the increase in AP

activity is largely affected by temperature. Coccolith production, however, was greatly stimulated at low temperatures the amount of $^{45}Ca$ incorporation was about five times higher at 12°C than at 20°C 6 d after exposure to cold stress. Notably, calcification was initiated about 1 d earlier than the induction of AP (Fig. I-2C). When *E. huxleyi* cells were suspended in the medium with sufficient-Pi and without addition of Pi, cell growth ceased about 3 and 2 d after the initiation of culture, respectively. The increase in AP activity that is due to *de novo* synthesis by Pi-limitation was obvious at 3 d in Pi-limited culture but very little in Pi-sufficient culture. Similarly, calcification, expressed as $^{45}Ca$-incorpotation, was stimulated in Pi-limited culture but no or less in Pi-sufficient culture (Fig. I-3A). The stimulation of AP activity and calcification caused by Pi deprivation was negated by the addition of phosphate to the medium following a transient increase in AP activity and a lag of several hours in calcification. (Fig. I-3B).

AP activity and $^{45}Ca$ incorporation for calcification clearly increased when cells were transferred to $P_i$-deficient conditions at low temperature (Fig. I-4). When cells were transferred from 20° to 12°C, cell growth rate was not significantly affected by $P_i$ availability. AP activity and calcification, however, were greatly stimulated by $P_i$-deficiency. $^{45}Ca$ incorporation increased slightly but then ceased altogether until day 3 at 12°C even under phosphate-sufficient conditions, although AP was not induced (Fig. I-4C). This suggests that cold stress itself may also function as a trigger for calcification since the calcification began prior to AP induction when the cells were exposed to both stressors. Calcification was primarily regulated by $P_i$ availability while cold stress functioned as a stimulating factor (Figs. I-3, -4).

The physiological data on coccolith production was confirmed by morphological observations under bright-field and polarizing microscopes (Fig. I-5). The cells in

logarithmic growth phase had almost no coccoliths and were approximately 3–4 μm in diameter (Fig. I-5B-a). When the culture was allowed to grow until it became $P_i$-deprived at constant temperature, the cells began to increase in size to 5 μm, but the production of coccoliths on the cell surface was very low (Fig. I-5B-b). In contrast, *E. huxleyi* transferred to low temperature (13°C) under $P_i$-deficient conditions increased its cell size and produced many coccoliths (Fig. I-5B-c). However, the cells grown at the lower temperature under phosphate-sufficient conditions produced no coccoliths on the cell surface, although cell size increased similarly to cells grown in Pi-deficient medium (Fig. I-5B-d). As *E. huxleyi* cells transferred to 13°C increased slightly in cell size (Fig. I-5B-d), the calcification process may be proceeding even though it is not yet observable under the microscope. These data demonstrate the significant stimulatory effect of cold stress on coccolith production in the coccolithophorid *E. huxleyi* under $P_i$-deficient conditions.

Discussions

**Relationship between $^{45}$Ca-Incorporation and Coccolith Production**

*E. huxleyi* is phylogenetically closely related to *Isochrysis galbana*, a non-coccolith-producing haptophyte (Edvardsen et al., 2000; Fujiwara et al., 2001). Our previous results demonstrated that incorporation of $^{45}$Ca by *I. galbana* was several hundred times less than that by *E. huxleyi* even though the cell sizes are nearly equivalent (Sorrosa et al., 2005). The data presented here in Figure I-1 confirm that $^{45}$Ca absorbed by *E. huxleyi* cells is primarily used for coccolith production and that only a tiny percentage of the $^{45}$Ca remains inside the cells themselves. This suggests that haptophyte algae require a high concentration of calcium only for calcification and calcium is primarily used for coccolith production and not for other cellular activities. Therefore, the total $^{45}$Ca incorporated by *E. huxleyi* can be thought of as a quantitative measure of coccolith production. Coccolith production by a coccolithophorid such as *E. huxleyi* was confirmed to be a mechanism for the storage of huge amounts of calcium and inorganic carbon.

**Relationship between Cold and Phosphate-deficient Stresses in Calcification by *E. huxleyi***

$P_i$ limitation is known to increase the ratio of carbon deposition into coccoliths produced by calcification to organic materials produced by photosynthesis, expressed as the C/P ratio (Paasche and Brubak, 1994; van Bleijswijk et al., 1994). Moreover, an increase in temperature from 10° to 15°C was reported to lead to a slight increase in the C/P ratio since calcification was stimulated and the production of organic matter was

slightly reduced (van Bleijswijk et al., 1994). By estimating calcification activity using the incorporation of $^{45}Ca$ into coccoliths, the present study clearly showed that $P_i$ deprivation induces both AP activity and coccolith production (Figs. I-2, -3), as previously observed by Paasche (1998) and Riegman et al. (2000). AP was shown to localize on the cell surface in *E. huxleyi* by biochemical and gene analyses (Landry et al., 2006; Xu et al., 2006). In addition, my results clearly show that coccolith production can be triggered by a low temperature signal prior to the AP induction when cells are exposed to the double stresses of cold and $P_i$ limitation (Fig. I-4). Calcification was greatly stimulated when both a cold stress and a $P_i$-deficient signal were given simultaneously (Figs. I-4, -5).

Figure 5 clearly indicates that the cell diameter increased when cells were placed under cold stress and $P_i$-deficient conditions. Sorrosa et al. (2005) also observed cell enlargement under cold stress but did not investigate $P_i$ limitation. A close relationship between cell enlargement and the stimulation of coccolith production was described previously (Shiraiwa, 2003; Sorrosa et al., 2005). Here I show that *E. huxleyi* coccolith production and cell size are strongly regulated by changes in environmental factors and growth status. During rapid cell division in the logarithmic growth phase, cells remained small in size without coccolith production on the cell surface (Fig. I-5). These results suggest that coccolith production may be important in less active cells, and a possible role of the coccolith production is to avoid stresses that may result in cell damage.

Cold stress on a plant leads to the modification of metabolism in two ways. The first is through a mechanism that improves stress tolerance, and the second adjusts metabolic processes to the consequences of cold stress (Guy et al., 2008). Cold stress is

known to induce the expression of a desaturase and to enhance the production of unsaturated fatty acids in order to increase membrane flexibility at low temperatures (Wada et al., 1994; Los et al., 1993; Los et al., 1997). In this case, the physiological function of the increase in the desaturase activity is very clear. The physiological importance of the stimulation of coccolith production under cold and $P_i$-deficient conditions, however, remains to be elucidated.

$P_i$ limitation generally induces the suppression of photosynthetic carbon metabolism by reducing the amount of phosphate compounds and the activities of some enzymes in the plastid $C_3$ cycle, including via ATP synthesis (Rao and Terry, 1989). Coccolith production occurs in a coccolith vesicle, a separate compartment considered to be derived from the Golgi apparatus and probably associated with the nuclear envelope during the initial stage of calcification in *E. huxleyi* (Westbroek et al., 1989; Pienaar, 1994; de Vrind-de Jong and de Vrind, 1997). Electron microscopy studies indicate that the coccolith vesicle disappears during cell division (Linschooten et al., 1991). The cessation or decrease in cell division may be needed to promote coccolith production, as suggested by previous reports (Paasche and Brubak, 1994; Paasche, 1998).

My study has suggested relationship between cold stress and $P_i$ deficiency in photosynthetic organisms; it showed that low temperatures lead to rapid accumulation of phosphorylated metabolites and the depletion of $P_i$ (Hurry et al., 1994). The intracellular status of phosphate metabolism is expected to integrate calcification via such processes. The intracellular status of phosphate should be investigated to elucidate the $P_i$-deficient induction of calcification.

The enhancement of coccolith production by low temperatures under $P_i$-limiting

conditions may be one of the key factors as to why coccolithophore blooms have been observed in the ocean at high latitudes where the temperature is low. Further studies are necessary to elucidate the detailed molecular mechanism that allows cold stress and Pi deficiency to regulate coccolith production. Studying the regulatory mechanisms will also provide insight into the physiological role of coccolithophorean coccoliths.

# Chapter II

Identification and Characterization of the Protein, EhFKBP21, Associated with Coccolith Production by *Emiliania huxleyi*

Summary

I found a protein synthesized specifically when coccolith production was enhanced. I purified the protein by acetone precipitation and anion exchange chromatography and characterized it. The molecular mass and pI of the protein experimentally determined were 32-kDa and 4.2, respectively. From the determined N-terminal amino acid sequence, a full-length deduced amino acid sequence was determined by homology search in both EST and genome databases of *E. huxleyi*. The sequence has a highly conserved FKBP-type peptidyl-prolyl *cis-trans* isomerase (PPIase) domain and the calculated molecular mass and pI are 21,767 and 4.7, respectively. I named the protein EhFKBP21. Some post-translational modification is expected because the calculated molecular mass and pI were different from those experimentally determined. The sequence had a signal peptide at the N-terminal and an ER retention sequence KDEL at the C-terminal. The sequence also contained two calcium-binding motifs (EF-hand motifs) at C-terminal side of FKBP-type PPIase domain. The addition of 1 μM FK506, an inhibitor of the binding of calcium to FKBP, affected neither the rate of growth nor calcium incorporation by *E. huxleyi* cells under Pi-deficient conditions where intracellular calcification is enhanced. Detailed function of the protein and its association with calcification remain to be clarified in future study.

## Introduction

*E. huxleyi* has heterococcoliths, formed of a radical array of complex-shaped calcite crystals. The coccoliths include small relict crystalline elements, such as overgrown coccoliths and proto-coccoliths composed of oval ring of rombohedra investigated in early phase of coccolith production (Young et al., 1992; Young et al., 1999). Strict cellular control over the calcification process is expected by the characteristic morphology of larger unit-crystal elements and by existence of two types of crystalline elements. Coccolith formation takes place in a dedicated intracellular calcifying vesicle that is closely associated with the nuclear envelope and a reticular body, a complex membrane system distally connected to the calcifying vesicle. It is expected that the coccolith-production compartment is formed by fusion of Golgi-derived vesicles (van der Wal et al., 1983; van Emburg et al., 1986). Process in stages of coccolith formation was extensively described by Westbroek (1989) and de Vrind-de Jong et al. (1994), as follows. First, an organic base plate is formed within the calcifying vesicle. The unit-crystal elements are nucleated on the rim of the organic base plate. While the crystals grow in specific directions to develop the final form of the unit elements, the calcifying vesicle expands to create room for the growing coccolith. Finally, the completed coccolith is extruded and incorporated in the coccosphere (FigII-1). Thus, the calcification of *E. huxleyi* is most likely to involve many organic molecules. In contrast to such mechanism for crystal formation of coccolith, the processes for the accumulation of calcium and dissolved inorganic carbon (DIC) are unknown yet although the active transport system of such substrates should be driven during coccolith production. In addition, the production of organic matters such as acid

polysaccharides associated with coccolith production as regulators (Marsh, 2003) also needs to be studied how those materials are synthesized and regulated in relation to the coccolith production process.

Research on genes and proteins associated with intracellular calcification in *E. huxleyi* is progressing. One protein was identified and named GPA for its high content of glutamic acid, proline and alanine. GPA was isolated from intracellular polysaccharide fraction and has been implicated in the process of calcification in *E. huxley*i (Corstjens et al., 1998). Surprisingly, there is no report on this protein to confirm the function of the protein in calcification. Quinn et al. (2006) identified 45 gene sequences that are most likely to be involved in calcification by use of microarray and RT-PCR. 37 of them increase and 8 of them decrease in calcifying strain and Pi. In those genes, γ-carbonic anhydrase, the one similar to ankyrin 2, and phosphate-repressible phosphate permease were described as possible candidates for relating to calcification. However, 30 of them showed no homolog description and 4 of them showed homology with only hypothetical proteins. An analysis performed by using macroarray on other coccolithophorid, *Pleurochrysis haptonemofera*, revealed that transcriptional products of 54 genes increased specifically in calcified-cells. However, 27 of them had no homolog description (Fujiwara et al., 2007). These obscure results on finding of possible candidates for calcification-associated proteins probably depend on unique mechanism of calcification in coccolithophorids as well as on lack of experimental knowledge about proteins involved in calcification of coccolithophorids. Information on the function of proteins is surely essential for the elucidation of the mechanism of calcification.

In this chapter, I attempted to open the trail for the elucidation of the molecular

mechanism in calcification and therefore tried to identify and characterize proteins synthesized *de novo* when coccolith production is stimulated. For the experiments, the knowledge obtained in Chapter I of this thesis was used for setting the optimum conditions that enhance coccolith production.

Material and Methods

## Organism and Culture Conditions

The coccolithophorid, *E. huxleyi* (Lohman) Hay & Mohler (NIES 837), Haptophyceae, was grown in artificial seawater (Marine Art SF; produced by Tomita Seiyaku Co., Ltd., Tokushima, formerly distributed by Senju Pharmaceutical Co., Osaka, Japan, and recently by Osaka Yakken Co. Ltd., Osaka) enriched with Erd–Schreiber's medium containing 10 nM sodium selenate instead of soil extracts (MA-ESM) (Danbara and Shiraiwa, 1999). Cells were maintained under constant illumination at 100 $\mu mol \cdot m^{-2} \cdot s^{-1}$ and 20°C (standard condition). Cells in early linear growth phase were transferred to 12° or 13°C for low temperature treatments. For Pi-deficient condition, cells in early linear growth phase were collected by weak centrifugation (550 × *g*, 10 min), washed with phosphate-free MA-ESM, resuspended in the fresh one.

## $^{45}$Ca Tracer Experiments for Calcification

First, 21 kBq/mL of $^{45}CaCl_2$ (27 GBq/mmol, Perkin-Elmer, Waltham, MA) was injected into cell culture to initiate the $^{45}$Ca-labeling reaction. At appropriate intervals 400 μL of culture was harvested by a centrifuge-filtration method using an Ultrafree-MC filter (pore size, 0.65 μm; Millipore, Billerica, MA). The filter with cells was brought into a vial containing 1.0 mL scintillation cocktail, Hionic-Fluor (Perkin-Elmer), to determine the radioactivity using a liquid scintillation counter (LS 5000TD; Beckman, Fullerton, CA).

## Metabolic Labeling and Detection of Labeled Proteins

An aliquot of cell culture was incubated with 1,480 Bq·mL$^{-1}$ of [$^{35}$S] methionine and cysteine ($^{35}$S-Met/Cys) Promix (GE Healthcare UK Ltd) for 1 h. $^{35}$S-labeled cells were harvested by centrifugation (5,000 × *g* for 5 min at the temperature the cells were incubated) and suspended in 50 mM tris (hydroxymethyl) aminomethane (Tris)-HCl, pH 7.0. The cells were disrupted by sonication, and the homogenate was centrifuged at 20,000 × *g* for 30 min at 4°C. The supernatant containing soluble proteins was analyzed using SDS-PAGE after acetone precipitation. $^{35}$S-labeled, *de novo* synthesized protein was visualized by radioluminography using a BAS 1800-II system (Fuji Film, Tokyo, Japan). The images were analyzed using ImageGauge 4.0 (Fuji Film, Tokyo, Japan).

In two-dimensional PAGE analysis, isoelectric focusing (IEF) was performed with the Pharmacia IPGphor System for the first dimensional development. Samples were treated using 2-D Clean-Up Kit (GE Healthcare UK Ltd) and resuspended in DeStreak Rehydration Solution (GE Healthcare UK Ltd) containing 0.5% (v/v) IPG buffer (GE Healthcare UK Ltd). The mixture was loaded on 7-cm IPG strips, pH 3-10 (GE Healthcare UK Ltd). For the second dimension, the IPG strips after IEF were applied to SDS-PAGE that was preformed on a 4 M urea-12.5% acrylamide gel. After electrophoresis the gels were stained with 2-D silver stain·II DAIICHI (Daiichi Pure Chemicals, Tokyo, Japan). The pI value was determined according to the standard curve provided by GE Healthcare UK Ltd.

**Purification of the Protein**

The water-soluble proteins were fractionated by acetone precipitation. After precipitation with 40% acetone, the 40%-acetone-soluble proteins were brought to precipitation with 75% acetone. The precipitates were resuspended in 10 mM

Tris-acetate, pH 7.0 (buffer A) and filtrated by using Ultrafree-MC filter unit (Millipore, Bedford, MA) to remove undissolved materials. The filtrate was applied to a TSKgel BioAssist Q (Tosoh Co., Tokyo, Japan) column that had been equilibrated with buffer A. After washing the column with 5 bed volumes of buffer A, proteins were eluted with 35 mL of buffer A with a linearly ascending gradient of $(NH_4)_2SO_4$ from 0 to 0.6 M at a flow rate of 1 mL·min$^{-1}$and fractionated 1 mL·fraction$^{-1}$. Each fraction was applied to SDS-PAGE and radioluminography.

For amino acid sequencing at a cold laboratory, non-radioactive protein samples should be prepared according to the same protocol that had been used to purify the $^{35}$S-labeled 32-kDa protein. To confirm the identity of the $^{35}$S -labeled and unlabeled protein, the mixture of both samples was loaded to 2D-IEF/SDS-PAGE and transferred to a polyvinylidene difluoride membrane. The Coomassie Brilliant Blue (CBB)-stained and radioactive protein band was compared and confirmed to be identical. After the confirmation, the CBB-stained band was used to analyze the N-terminal amino acid sequence by Edman degradation using a model 492cLC, Procise® cLC sequencing system (Applied Biosystems, Foster City, CA) at the National Institute for Basic Biology (Okazaki, Japan).

**Bioinformatic Analyses of the Protein**

A sequence search with *Emiliania* EST database (Wahlund et al., 2004) was performed using the BLAST algorithm, tblastn, from the National Center for Biotechnology Information (NCBI, http://www.ncbi.nlm.nih.gov/). *E. huxleyi* CCMP1516 genome was released from the Joint Genome Institute (JGI, http://www.jgi.doe.gov/) and a sequence search was also performed by using BLASTP

program (Altschul et al., 1997) with relaxed parameter (expect=$1e^{-5}$ was lowered to expect=5). The protein family signature was analyzed using the PROSITE database of protein families and domains (Hulo et al., 2007). The theoretical molecular weights of proteins were calculated using the calculation tool on the ExPaSy server (http://expasy.org/tools/pi_tool.html). A multiple alignment analysis and a secondary structure prediction were carried out using the Clustal W (Thompson et al., 1994) and Jpred (Cole et al., 2008), respectively. Signal peptide cleavage sites were identified by SignalP program (Bendtsen et al., 2004).

**Inhibitor Test**

FK506 was purchased from Cayman Chemical Co. (Ann Arbor, MI), and was diluted in methanol at concentration of 1 mM. *E. huxleyi* cells were transferred to phosphate-free medium at 0 h and then FK506 was added after 2 d incubation (final concentration, 1 μM).

Results

**Identification of Proteins Synthesized *de novo* in Accordance with the Stimulation of Coccolith Production**

*E. huxleyi* cells were transferred into the Pi-sufficient or -deficient conditions. Calcification activity monitored by $^{45}$Ca incorporation gradually increases after 2 d and rapidly accelerated after 4 d under Pi-deficient conditions (Fig. II-2A). After 4 d (96 h), $^{35}$S-Cys/Met was added to cells under Pi-deficient conditions and incubated 1 h for $^{35}$S-labeling, as described in **Materials and Methods**. Six proteins with molecular masses of 106, 84, 43, 32, 28 and 26-kDa were obviously increased under Pi-deficient conditions in comparison with Pi-sufficient conditions (Fig. II-2B). Among them, the most obvious band that showed the increase in $^{35}$S-activity under Pi-deficient condition was the 32-kDa band.

To enhance the calcification, cells were grown in the Pi-deficient medium for 69 h, and then dibasic potassium phosphate (final concentration, 28.7 μM) was added to the culture. Figure II-3A clearly shows that the enhancement of calcification by Pi-deficiency was quickly negated by Pi-addition. Under such conditions, 4 of the 6 proteins in Figure II-2B were reduced by the addition of phosphate. Those were 106, 43, 32 and 26-kDa proteins (Fig. II-3B). Among them, the most obvious change in $^{35}$S-labeling was observed in 32-kDa protein.

Figure II-4A clearly shows that calcification monitored by $^{45}$Ca incorporation into coccoliths was enhanced when the cells were transferred from 20°C to 12°C. The increase in calcification by low temperature showed an about 2 d lag and then obviously stimulated. Simply, there was almost no difference in calcification at 44.5 h (ca. 2 d)

(for $^{35}$S-labeling pattern at 12°C, see lane #1 in Fig. II-4B), but at 139 h (ca. 5.8 d) calcification was 5.6 times larger at 12°C than 20°C (for $^{35}$S-labeling pattern at 20°C and 12°C, see lane #2 and 3 in Fig. II-4B). $^{35}$S-labeling of 106, 43 and 26-kDa protein did not reflect the stimulation of calcification by low temperature, but only 32-kDa protein showed obvious change by stimulation at low temperature (Fig. II-4B).

**Purification of the 32-kDa Proteins**

First, the $^{35}$S-labeled 32-kDa protein was partially purified, as described in **Materials and Methods**. The protein was obtained in 40–75% acetone fraction (lane 2) and 60% acetone precipitates (lane 3), but not in 60–70% acetone fraction, showing that the best recovery could be obtained in 40–60% acetone fraction (Fig. II-5A). The proteins in 40–60% acetone fraction were applied to anion-exchange chromatography (Fig. II-5B). Most of radioactivity was eluted between Fraction 14 and Fraction 25 and the subpeaks of $^{35}$S-radioactivity were obtained in Fraction #17 and 20 (Fig. II-5B). SDS-PAGE analysis revealed that Fraction #16 contained the 32-kDa protein (Fig. II-5C).

Two-dimensional IEF/SDS-PAGE patterns were compared among samples from Pi-deficient culture cells and 12°C grown cells in which calcification is stimulated (Fig. II-6). Finally, 32-kDa proteins produced by Pi-deficient cells and cold-acclimated cells were identical not only in its mass but also in its isoelectric point (pI=4.2) (Fig. II-6C), suggesting that the proteins were identical.

**Sequence Analyses and Identification of the Protein, EhFKBP21**

The N-terminal amino acid sequence of the 32-kDa protein was determined by the

Edman degradation (Table II-1). The protein fragment consisted of 13 residues was used to obtain the information of full-length amino acid sequence. Four sequences were searched in EST database, and two sequences were searched in genome database (Table II-2). The two nucleotide sequences in genome database were identical when those were compared in deduced amino acid sequences. The deduced amino acid sequence with a molecular mass of 21,767-Da contained a FK506 binding protein (FKBP) type peptidyl-prolyl *cis-trans* isomerase (PPIase) domain, and therefore I named the protein EhFKBP21. PPIase (also known as rotamase; EC 5.2.1.8) catalyses the isomerization of the peptide bond by the modification of proline and the change finally induces structural change of protein. A homology search using the full-length EhFKBP21 revealed that the protein had strong sequence similarity to FKBPs belonging to insects, for example, *Drosophila melanogaster* FKBP13 (expected=$3\times e^{-42}$). EhFKBP21 included a hydrophobic signal peptide of 14 amino acids, which was expected to cleavage just before N-terminal region identified experimentally. EhFKBP21 also possessed an ER-retaining signal sequence of KDEL at C-terminal. From these two results, EhFKBP21 was predicted to locate in ER. The calculated molecular mass and pI of the mature protein were 20,493-Da and 4.7, respectively. Therefore, I expected that there are some post-translational modifications since there was the difference in molecular mass between theoretically estimated from deduced amino acid sequence and experimentally determined by SDS-PAGE. EhFKBP21 also possessed two EF-hand calcium-binding domains downstream of FKBP conserved domain. Second structure of the protein was predicted to involve 6 β-sheets and an α-helix upstream of EF-hand motifs. The α-helix was present between 4th β-sheet and 5th (Fig. II-7). FKBP-type PPIase domain was present in EhFKBP21 at position 39–134 (length of 96 aa). The

sequence identities of the domain and PPIase domains of other FKBP members that locate in ER is 56% with *Arabidopsis thaliana* FKBP15-2 (AtFKBP15-2), 48% with *Chlamydomonas reinhardtii* FKBP15-2 (FKB15-2), 55% with *Drosophila melanogaster* FKBP13 (DmFKBP13) and 37% with mouse FKBP23 (mFKBP23) (Fig. II-8A). The first two FKBPs in photoautotrophs did not possess EF-hand motifs, but the last two FKBPs in animals did. The identity of FKBP-type PPIase domain of EhFKBP21 to human FKBP12 (hFKBP12) atomic structure was 46%. The length of the conserved domain of EhFKBP21 was seven residues longer than that of hFKBP12 and the residues located at position 52–58. According to van Duyne et al. (1991), five amino acids within the conserved FK506 domain of FKBP12 are involved in hydrogen bonds between FKBP and FK506; $Ile^{56}$, $Glu^{54}$, $Gln^{53}$, $Asp^{37}$ and $Tyr^{82}$ (amino positions numbered after FKBP full-length sequence). The $Glu^{54}$ and $Gln^{53}$ residues are replaced by Arg and Gly, respectively, in EhFKBP21. These replacements are also found in the other FKBPs; namely, the $Glu^{54}$ is replaced by Gln in AtFKBP15-2, FKB15-2 and DmFKBP13, by His in mFKBP23, the $Gln^{53}$ is replaced by Gly in AtFKBP15-2, mFKBP23 and DmFKBP13 as like EhFKBP21. The side chains of $Tyr^{26}$, $Phe^{46}$, $Phe^{99}$, $Val^{55}$ and $Ile^{56}$ form the pocket that surrounds the FK506 binding site while $Trp^{59}$ is at the end of the pocket and serves as a platform for the pipecolinyl ring of FK506 (van Duyne et al., 1991). These residues are completely conserved in all of the FKBPs, except that $Phe^{46}$ is replaced by Ile in FKB15-2 and Lys in mFKBP23. Motif search analysis also revealed that the protein has two EF-hand motifs downstream of the PPIase motif. EF-hand motif possesses general feature of high-affinity $Ca^{2+}$-binding, i. e., the presence of helix-loop-helix motif which has five residues containing oxygen and the highly-conserved central glycine (Kretsinger, 1980; Moncrief, 1990). Although the

central glycine of the first motif was replaced by alanine, such replacement has been reported in other $Ca^{2+}$-binding proteins like mFKBP23, therefore this domain may also have $Ca^{2+}$ binding ability (Fig. II-8B).

**Effect of FK506 on *E. huxleyi***

The effects of FK506, an inhibitor of FKBP, on growth and calcification of *E. huxleyi* were analyzed. The cells grown in Pi-sufficient medium were transferred to Pi-deficient condition to stimulate coccolith production and incubated for 4 d at 20°C, and after 2 d incubation, 1 μM FK506 was added. There was no significant effect of FK506 on cell growth and coccolith production monitored by $^{45}Ca$-incorporation (Fig. II-9).

## Discussion

I identified a protein, FKBP, of which synthesis increased when coccolith production was enhanced by both Pi-deficiency and cold stress (Fig. II-2 to -7). FKBPs, cyclophilins (CyPs) and parvulins, represent three structurally unrelated classes of immunophilins that are known to function as PPIase (Schiene and Fischer, 2000). CyPs and parvulins are distinguished by their ability to bind different immunosuppressant drugs, either FK506/rapamycin or cyclosporin A. EhFKBP21 has two EF-hand motifs downstream of the FKBP-type PPIase domain and expected to possess $Ca^{2+}$-binding activity. According to investigation of many proteins which possess the EF-hand motif, one of the functions of EF-hand is intracellular $Ca^{2+}$ buffering associated with calcium transport and another is the regulation of enzyme activity (Weinstein and Mehler, 1994). This study is the first report on FKBP in *E. huxleyi* and on the regulation of the *de novo* synthesis of FKBP associated with coccolith production under Pi-deficiency and cold stress conditions. Both weak staining and strong labeling of EhFKBP21 by the silver-staining and $^{35}S$, respectively, suggest that the amount of the protein is very small but its turnover rate would be fast. Some post-translational modifications are expected in EhFKBP21since the experimentally determined molecular mass (32-kDa) and pI (4.2) of EhFKBP21 were so different from those calculated from its deduced amino acid sequence, 21.8-kDa and 4.7, respectively.

PPIases are widely found in various organisms and are present in all the major compartment of the cell to be involved in various processes like cell signaling, protein trafficking and transcription (Galat, 1993; Harrar et al., 2001), but there are few reports on PPIases in algae. Genes encoding PPIases are known in a green alga, *C. reinhardtii*

(Vallon, 2005), but FKBPs with EF-hand motif have not been reported in algae yet. In coccolithophorids, a transcriptional product of PPIase was reported to decrease under Pi-deficient condition in *E. huxleyi* (Quinn et al., 2006). CyPs and parvulins tend to be largely conserved in different species, but FKBPs do not. Thus it is suggested that CyPs and parvulins have evolved to perform conserved functions, but the FKBPs relatively have evolved to fill ever-changing niches within the constantly evolving organisms (Pemberton and Kay, 2005). *E. huxleyi* possesses subcellular calcification ability associated with specific membrane systems. This suggests that *E. huxleyi* may have specific FKBPs.

There is no effect of FK506 at 1 μM on the growth and the calcification by *E. huxleyi* (Fig. II-9). FK506 inhibits the PPIase activity of FKBPs (Heitman et al., 1991) and the range of effective concentrations varies from nanomolar to hundreds micromolar levels. Human FKBP12 shows a high affinity for FK506 (Ki = 0.6±0.2 nM) (Aldape et al., 1992). Mixed lymphocyte reaction is inhibited by 10 nM FK506 and cloned T-cell proliferation is completely inhibited 0.4 nM FK506 (Sawada et al., 1987). On the other hand, it is reported that PPIase activity of mFKBP60 was inhibited only in the presence of a very high concentration of FK506 (200 μM, it is more than a thousand times larger than the mFKBP60 concentration used in the experiment) *in vitro* assay (Shadidy et al., 1999). The higher inhibitory concentration is anticipated to be caused by the lack of conservation of some amino acid positions in the PPIase domains of mFKBP60 that are involved in FK506 binding in hFKBP12. *In vivo*, the growth of *Saccharomyces cerevisiae* suppresses in the presence of 62 μM FK506 but not in 31 μM FK506, and a human FKBP12 homolog, FPR1 is involved in the suppression (Heitman et al., 1991). EhFKBP21 has a longer PPIase domain and lacks two amino acids

involved in hydrophobic bonds between FKBP and FK506 (Fig. II-8A). Thus it is possible that the FK506 concentration used in this study was too low to induce some inhibitory effects on *E. huxleyi*. It is difficult to test effect of higher FK506 on *E. huxleyi* because of the low solubility of FK506 in water.

Mouse FKBP23 has a FKBP-type PPIase domain and a couple of EF-hand motifs like EhFKBP21 and binds to immunoglobulin heavy-chain-binding protein (BiP) and the binding is $Ca^{2+}$ dependent (Nakamura et al., 1998; Zhang et al., 2004). Mouse BiP is one of members of the Hsp70 family which has weak ATPase activity and functions as a chaperon, and the activity is inhibited by binding with mFKBP23 (Wang et al., 2007). As EhFKBP21 is a mFKBP23 homolog, it is possible to bind chaperon protein in $Ca^{2+}$ depending manner. *Neurospora crassa* FKBP22 also locates in ER, functionally cooperates with BiP, associates with several chaperones and folding catalysts and make complexes (Tremmel et al., 2007; Tremmel and Tropschug, 2007). Thus, it is also possible that EhFKBP21 associates with several proteins containing BiP.

In conclusion, I identified EhFKBP21 that was especially produced during coccolith production and of which the production was stimulated by Pi-deficiency and cold stress. The protein is expected to be involved in the quality maintenance system such as the holding mechanism of proteins in ER in $Ca^{2+}$ depending manner and to be associated with several proteins. It seems that a kind of quality maintaining system of proteins is stimulated during coccolith production. Investigation of protein network involving EhFKBP21 would lead the elucidation of intracellular process on coccolith production.

## General Discussion

In this thesis, I investigated that culture conditions and periods for stimulating coccolith production, focusing on phosphate deficiency and low temperature, and concluded that phosphate deprivation is the primary factor for stimulating coccolith production, and cold stress is the secondary factor to enhance the calcification. Upwelling current is likely to be a main supplier of nutrients in oceanic region and the temperature of such upwelling water is lower than that of surface water. Phosphate concentration is very low at micromolar level in the ocean (Yoshimura et al., 2007; Kamykowski, 2008) and the concentration much lower than that of culture medium used for the culture of *E. huxleyi*. Under such conditions where *E. huxleyi* is relatively dominant, phosphate that supplied by upwelling current is deprived for a second and the effect of phosphate deprivation and cold water would trigger calcification and it makes *E. huxleyi* bloom visible from the satellite. I also found a protein that is synthesized *de novo* when coccolith production was stimulated both under Pi-deficient and low temperature conditions in this study. A homology search of the deduced amino acid sequence of the protein suggested that the protein is homologous to FKBP and therefore I named the protein EhFKBP21. Most possible function of EhFKBP21 is expected to function in folding and processing of proteins in ER by its predicted localization and the presence of FKBP-type PPIase domain. FKBPs generally associate and regulate partner proteins, although the partner proteins remain to be identified in algae.

The function of FKBPs in unicellular organisms is still quite unclear in spite of widespread distribution of the proteins among organisms. In *S. cerevisiae*, individual and collective deletion of FKBPs does not affect the viability and it does not suggest

FKBPs play an essential general role (Dolinski et al., 1997). It has been shown that a FKBP located in ER, FKBP13, is up-regulated by accumulation of unfolded proteins (Partaledis and Berlin, 1993; Bush et al., 1994). Similar regulation system is expected to other FKBPs which locate and associate with mature process of proteins in ER. Calcification is enhanced by some stressful conditions which may cause accumulation of immature protein. Most popular function of FKBPs in ER is to act as chaperone. Further experiments are necessary to analyze molecular mechanism how *de novo* synthesis of EhFKBP21 regulates coccolith production. The relationship between coccolith producing mechanism and the function of EhFKBP21 is unknown yet, but they are possible to share some regulating systems. The elucidation of the regulatory mechanism of EhFKBP21 may give important information on regulation of coccolith production.

Coccolith production by coccolithophorids requires the intracellular accumulation of calcium, bicarbonate ions and organic base plate in the coccolith vesicles. Brownlee et al. (1994) calculated that the net influx of $Ca^{2+}$ across the plasma membrane of calcifying *E. huxleyi* cells is 3–5 $pmol \cdot cm^{-2} \cdot s^{-1}$ which is relatively higher than that of other plants and marine algae. Because the cytosolic free $[Ca^{2+}]$ in *E. huxleyi* is as low as other organisms (Brownlee et al., 1995), there would be $Ca^{2+}$ transport pathway which does not disturb general calcium signaling. However, from its uptake to accumulation into the coccolith vesicles, there are few reports about the $Ca^{2+}$ transport systems in *E. huxleyi*. If ER is involved in the $Ca^{2+}$ transport systems in *E. huxleyi*, it would be possible that EhFKBP21 is affected by change in $[Ca^{2+}]$ that is accompanied with the enhancement of calcification.

For further investigation of the relationship between the coccolith production and

the function of EhFKBP21, experimentally determined localization of the protein would be important. *E. huxleyi* has specific membrane systems of which origin are still unknown. If EhFKBP21 is associated with membrane system which involved in coccolith production, it is possible that EhFKBP21 plays a role in coccolith production.

References

Aldape RA, Futer O, DeCenzo MT, Jarrett BP, Murcko MA, Livingston DJ (1992) Charged surface residues of FKBP12 participate in formation of the FKBP12-FK506-calcineurin complex. J Biol Chem 267, 16029–16032

Altschul SF, Madden TL, Schäffer AA, Zhang J, Zhang Z, Miller W, Lipman DJ (1997) Gapped BLAST and PSI-BLAST: a new generation of protein database search programs. Nucleic Acids Res 25, 3389–3402

Araki Y, González EL (1998) V- and P-type $Ca^{2+}$-stimulated ATPases in a calcifying strain of *Pleurochrysis* sp. (Haptophyceae). J Phycol 34, 79–88

Baeuerlein E (2000) Biominerals – an introduction. In: *Biomineralization*, Baeuerlein E (ed) WILEY-VCH, Weinheim, Germany, pp. 1–3

Bendtsen JD, Nielsen H, von Heijne G, Brunak S (2004) Improved prediction of signal peptides: SignalP 3.0. J Mol Biol 340, 783–795

Brassell SC, Eglinton G, Marlowe IT, Pflaumann U, Sarnthein M (1986) Molecular stratigraphy: a new tool for climatic assessment. Nature 320, 129–133

Brownlee C, Nimer N, Dong LF, Merrett MJ (1994) Cellular regulation during calcification in *Emiliania huxleyi*. In: *The Haptophyte Algae*, Green JC, Leadbeater

BSC (eds) Oxford, UK, pp. 133–148

Brownlee C, Davies M, Nimer N, Dong LF, Merrett MJ (1995) Calcification, photosynthesis and intracellular regulation in *Emiliania huxleyi*. Bull Inst Oceanogr Monaco 14, 19–35

Bush KT, Hendrickson BA, Nigam SK (1994) Induction of the FK506-binding protein, FKBP13, under conditions which misfold proteins in the endoplasmic reticulum. Biochem J 303, 705–708

Cole C, Barber JD, Barton GJ (2008) The Jpred 3 secondary structure prediction server. Nucleic Acids Res W197–W201

Corstjens PLAM, van der Kooij A, Linschooten C, Brouwers GJ, Westbroek P, de Vrind-de Jong EW (1998) GPA, a calcium-binding protein in the coccolithophorid *Emiliania huxleyi* (Prymnesiophyceae). J Phycol 34, 622–630

Corstjens PLAM, Araki Y, González EL (2001) A coccolithophorid calcifying vesicle with a vacuolar-type ATPase proton pump: Cloning and immunolocalization of the $V_0$ subunit $c^1$. J Phycol 37, 71–78

Corstjens PLAM, González EL (2004) Effects of nitrogen and phosphorus availability on the expression of the coccolith-vesicle V-ATPase (subunit *c*) of *Pleurochrysis* (Haptophyta). J Phycol 40, 82–87

Danbara A, Shiraiwa Y (1999) The requirement of selenium for the growth of marine coccolithophorids, *Emiliania huxleyi*, *Gephyrocapsa oceanica* and *Helladosphaera* sp. (Prymnesiophyceae). Plant Cell Physiol 40, 762–766

de Vrind-de Jong EW, van Emburg PR, de Vrind JPM (1994) Mechanism of calcification: *Emiliania huxleyi* as a model system. In: *The Haptophyte Algae*, Green JC, Leadbeater BSC (eds) Oxford, UK, pp. 149–166

de Vrind-de Jong EW, de Vrind JPM (1997) Algal deposition of carbonates and silicates. In: *Geomicrobiology*: *Interactions between Microbes and Minerals*, Banfield JF, Nealson KH (eds) The Mineralogical Society of America, Washington, DC, pp. 267–307

Dolinski K, Muir S, Cardenas M, Heitman J (1997) All cyclophilins and FK506 binding proteins are, individually and collectively, dispensable for viability in *Saccharomyces cerevisiae*. Proc Natl Acad Sci USA 94, 13093–13098

Dyhrman ST, Palenik B (1999) Phosphate stress in cultures and field populations of the dinoflagellate *Prorocentrum minimum* detected by a single-cell alkaline phosphatase assay. Appl Environ Microbiol 65, 3205–3212

Dyhrman ST, Palenik B (2003) Characterization of ectoenzyme activity and phosphate-regulated proteins in the coccolithophorid *Emiliania huxleyi*. J Plankton Res

25, 1215–1225

Edvardsen B, Eikrem W, Green JC, Andersen RA, Moon-van der Staay SY, Medlin LK (2000) Phylogenetic reconstructions of the Haptophyta inferred from 18S ribosomal DNA sequences and available morphological data. Phycologia 39, 19–35

Fichtinger-Schepman AMJ, Kamerling JP, Vliegenthart JFG, de jong EW, Bosch L, Westbroek P (1979) Composition of a methylated, acidic polysaccharide associated with coccoliths of *Emiliania huxleyi* (Lohmann) Kamptner. Carbohydr Res 69, 181–189

Fichtinger-Schepman AMJ, Kamerling JP, Versluis C, Vliegenthart JFG (1980) Structural analysis of acidic oligosaccharides derived from the methylated, acidic polysaccharide associated with coccoliths of *Emiliania huxleyi* (Lohmann) Kamptner. Carbohydr Res 86, 215–225

Fichtinger-Schepman AMJ, Kamerling JP, Versluis C, Vliegenthart JFG (1981) Structural studies of the methylated, acidic polysaccharide associated with coccoliths of *Emiliania huxleyi* (Lohmann) Kamptner. Carbohydr Res 93, 105–123

Fujiwara S, Tsuzuki M, Kawachi M, Minaka N, Inouye I (2001) Molecular phylogeny of the Haptophyta based on the *rbc*L gene and sequence variation in the spacer region of the RUBISCO operon. J Phycol 37, 121–129

Fujiwara S, Hirokawa Y, Takatsuka Y, Suda K, Asamizu E, Takayanagi T, Shibata D,

Tabata S, Tsuzuki M (2007) Gene expression profiling of coccolith-bearing cells and naked cells in haptophyte *Pleurochrysis haptonemofera* with a cDNA macroarray system. Mar Biothecnol 9, 550–560

Galat A (1993) Peptidylproline *cis*-*trans*-isomerases: immunophilins. Eur J Biochem 216, 689–707

Green JC, Heimdal BR, Paasche E, Moate R (1998) Changes in calcification and the dimensions of coccoliths of *Emiliania huxleyi* (Haptophyta) grown at reduced salinities. Phycologia 37, 121–131

Guy C, Kaplan F, Kopka J, Selbig J, Hincha DK (2008) Metabolomics of temperature stress. Physiol Plant 132, 220–235

Harrar Y, Bellini C, Faure JD (2001) FKBPs: at the crossroads of folding and transduction. Trends Plant Sci 6, 426–431

Heitman J, Movva NR, Hiestand PC, Hall MN (1991) FK 506-binding protein proline rotamase is a target for the immunosuppressive agent FK 506 in *Saccharomyces cerevisiae*. Proc Natl Acad Sci USA 88, 948–1952

Hirokawa Y, Fujiwara S, Tsuzuki M (2005) Three types of acidic polysaccharides associated with coccolith of *Pleurochrysis haptonemofera*: Comparison with *Pleurochrysis carterae* and analysis using fluorescein-isothiocyanate-labeled lectins.

Mar Biotechnol 7, 634–644

Hoppe HG (2003) Phosphatase activity in the sea. Hydrobiologia 493,187–200

Hulo N, Bairoch A, Bulliard V, Cerutti L, Cuche BA, de Castro E, Lachaize C, Langendijk-Genevaux PS, Sigrist CJA (2007) The 20 years of PROSITE. Nucleic Acids Res 36, D245–D249

Hurry VM, Malmberg G, Gardestöm P, Öquist G (1994) Effect of short-term shift to low temperature and of long-term cold hardening on photosynthesis and ribulose 1,5-bisphosphate carboxylase/oxygenase and sucrose phosphate synthase activity in leaves of winter rye (*Secale cereale* L.). Plant Physiol 106, 983–990

Kamykowski D (2008) Estimating upper ocean phosphate concentrations using ARGO float temperature profiles. Deep-Sea Res I 55, 1580–1589

Kretsinger RH (1980) Crystallographic studies of calmodulin and homologs. Ann N Y Acad Sci 356, 14–19

Landry DM, Gaasterland T, Palenik BP (2006) Molecular characterization of a phosphate-regulated cell-surface protein from the coccolithophorid, *Emiliania huxleyi* (Prymnesiophyceae). J Phycol 42, 814–821

Linschooten C, van Bleijswijk JDL, van Emburg PR, de Vrind JPM, Kempers ES,

Westbroek P, de Vrind-de Jong EW (1991) Role of the light–dark cycle and medium composition on the production of coccoliths by *Emiliania huxleyi* (Haptophyceae). J Phycol 27, 82–86

Los D, Horvath I, Vigh L, Murata N (1993) The temperature-dependent expression of the desaturase gene *desA* in *Synechocystis* PCC6803. FEBS Lett 318, 57–60

Los DA, Ray MK, Murata N (1997) Differences in the control of the temperature-dependent expression of four genes for desaturases in *Synechocystis* sp. PCC 6803. Mol Microbiol 25, 1167–1175

Marsh ME (2003) Regulation of $CaCO_3$ formation in coccolithophores. Comp Biochem Physiol 136B, 743–754

Marsh ME, Chang DK, King GC (1992) Isolation and characterization of a novel acidic polysaccharide containing tartrate and glyoxylate residues from the mineralized scales of a unicellular coccolithophorid alga *Pleurochrysis carterae*. J Biol Chem 267, 20507–20512

Moncrief ND, Kretsinger RH, Goodman M (1990) Evolution of EF-hand calcium-modulated proteins. I. Rerationships based on amino acid sequences. J Mol Evol 30, 522–562

Murphy J, Riley JP (1962) A modified single solution method for the determination of

phosphate in natural waters. Anal Chim Acta 27, 31–36

Nakamura T, Yabe D, Kanazawa N, Tashiro K, Sasayama S, Honjo T (1998) Molecular cloning, characterization, and chromosomal localization of FKBP23, a novel FK506-binding protein with $Ca^{2+}$-binding ability. Genomics 54, 89–98

Okada H, McIntyre A (1979) Seasonal distribution of modern coccolithophores in the western North Atlantic Ocean. Mar Biol 54, 319–328

Ozaki N, Sakuda S, Nagasawa H (2001) Isolation and some characterization of an acidic polysaccharide with anti-calcification activity from coccoliths of a marine alga, *Pleurochrysis carterae*. Biosci Biotec Biochem 65, 2330–2333

Paasche E (1964) A tracer study of the inorganic carbon uptake during coccolith formation and photosynthesis in the coccolithophorid *Coccolithus huxleyi*. Physiol Plant Suppl 3, 1–82

Paasche E (1998) Roles of nitrogen and phosphorous in coccolith formation in *Emiliania huxleyi* (Prymnesiophyceae). Eur J Phycol 33, 33–42

Paasche E (2002) A review of the coccolithophorid *Emiliania huxleyi* (Prymnesiophyceae), with particular reference to growth, coccolith formation, and calcification–photosynthesis interactions. Phycologia 40, 503–529

Paasche E, Brubak S (1994) Enhanced calcification in the coccolithophorid *Emiliania huxleyi* (Haptophyceae) under phosphorus limitation. Phycologia 33, 324–330

Paasche E, Brubak S, Skattebøl S, Young JR, Green JC (1996) Growth and calcification in the coccolithophorid *Emiliania huxleyi* (Haptophyceae) at low salinities. Phycologia 35, 394–403

Partaledis JA, Berlin V (1993) The *FKB2* gene of *Saccharomyces cerevisiae*, encoding the immunosuppressant-binding protein FKBP-13, is regulated in response to accumulation of unfolded proteins in the endoplasmic reticulum. Proc Natl Acad Sci USA 90, 5450–5454

Pemberton TJ, Kay JE (2005) Identification and comparative analysis of the peptidyl-prolyl *cis/trans* isomerase repertoires of *H. sapiens*, *D. melanogaster*, *C. elegans*, *S. cerevisiae* and *Sz. Pombe*. Comp Funct Genom 6, 277–300

Perry MJ (1972) Alkaline phosphatase activity in subtropical Central North Pacific waters using a sensitive fluorometric method. Mar Biol 15, 113–119

Pienaar RN (1994) Ultrastructure and calcification of coccolithophores. In: *Coccolithophores*, Winter A, Siesser WG (eds) Cambridge University Press, Cambridge, UK, pp. 13–37

Prahl FG, Wakeham SG (1987) Calibration of unsaturation patterns in long-chain ketone

compositions for palaeotemperature assessment. Nature 330, 397–369

Quinn P, Bowers RM, Zhang X, Wahlund TM, Fanelli MA, Olsozova D, Read BA (2006) cDNA microarrays as a tool for identification of biomineralization proteins in the coccolithophorid *Emiliania huxleyi* (Haptophyta). Appl Environ Microbiol 72, 5512–5526

Rao IM, Terry N (1989) Leaf phosphate status, photosynthesis, and carbon partitioning in sugar beet: I. Changes in growth, gas exchange, and Calvin cycle enzymes. Plant Physiol 90, 814–819

Reichardt W, Overbeck J, Steubing L (1967) Free dissolved enzymes in lake waters. Nature 216, 1345–1347

Riegman R, Stolte W, Noordeloos AAM, Slezak D (2000) Nutrient uptake, and alkaline phosphatase (EC 3: 1: 3: 1) activity of *Emiliania huxleyi* (Prymnesiophyceae) during growth under N and P limitation in continuous cultures. J Phycol 36, 87–96

Sawada S, Suzuki G, Kawase T, Takaku F (1987) Novel immunosuppressive agent, FK506 in vitro effects on cloned T cell activation. J Immunol 139, 1797–1803

Schiene C, Fischer G (2000) Enzymes that catalyse the restructuring of proteins. Curr Opin Struc Biol 10, 40–45

Shadidy M, Caubit X, Olsen R, Seternes OM, Moens U, Krauss S (1999) Biochemical analysis of mouse FKBP60, a novel member of the FKBP family. Biochim Biophys Acta 1446, 295–307

Shiraiwa Y (2003) Physiological regulation of carbon fixation in the photosynthesis and calcification of coccolithophorids. Comp Biochem Physiol 136B, 775–783

Sorrosa JM, Satoh M, Shiraiwa Y (2005) Low temperature stimulates cell enlargement and intracellular calcification of coccolithophorids. Mar Biotechnol 7, 128–133

Takano H, Takei R, Manabe E, Burgess JG, Hirano M, Matsunaga T (1995) Increased coccolith production by *Emiliania huxleyi* cultures enriched with dissolved inorganic carbon. Appl Microbiol Biotechnol 43, 460–465

Thompson JD, Higgins DG, Gibson TJ (1994) CLUSTAL W: improving the sensitivity of progressive multiple sequence alignment through sequence weighting, position-specific gap penalties and weight matrix choice. Nucleic Acids Res 22, 4673–4680

Tremmel D, Duarte M, Videira A, Tropschug M (2007) FKBP22 is part of chaperone/folding catalyst complexes in the endoplasmic reticulum of *Neurospora crassa*. FEBS Let 581, 2036–2040

Tremmel D, Tropschug M (2007) *Neurospora crassa* FKBP22 is a novel ER chaperone

and functionally cooperates with BiP. J Mol Biol 369, 55–68

Trimborn S, Langer G, Rost B (2007) Effect of varying calcium concentrations and light intensities on calcification and photosynthesis in *Emiliania huxleyi*. Limnol Oceanogr 52, 2285–2293

Vallon O (2005) *Chlamydomonas* immunophilins and parvulins: survey and critical assessment of gene models. Eukaryotic Cell 4, 230–241

van Bleijswijk JDL, Kempers RS Veldhuis MJ (1994) Cell and growth characteristics of types A and B of *Emiliania huxleyi* (Prymnesiophyceae) as determined by flow cytometry and chemical analyses. J Phycol 30, 230–241

van der Wal P, de Jong EW, Westbroek P (1983) Ultrastructural polysaccharide localization in calcifying and naked cells of the coccolithophorid *Emiliania huxleyi.* Protoplasma 118, 157–168

van Duyne GD, Standaert RF, Karplus PA, Schreiber SL, Clardy J (1991) Atomic structure of FKBP–FK506, an immunophilin–immunosuppressant complex. Science 252, 839–842

van Emburg PR, de Jong EW, Daems WT (1986) Immunochemical localization of a polysaccharide from biomineral structures (coccoliths) of *Emiliania huxleyi*. J Ultrastruct Mol Struct Res 94, 246–259

Wada H, Gombos Z, Murata N (1994) Contribution of membrane lipids to the ability of the photosynthetic machinery to tolerate temperature stress. Proc Natl Acad Sci USA 91, 4273–4277

Wahlund TM, Hadaegh AR, Clark R, Nguyen B, Fanelli M, Read BA (2004) Analysis of expressed sequence tags from calcifying cells of marine coccolithophorid (*Emiliania huxleyi*). Mar Biotechnol 6, 278–290

Wang Y, Han RF, Wu D, Li J, Chen C, Ma H, Mi HF (2007) The binding of FKBP23 to BiP modulates BiP's ATPase activity with its PPIase activity. Biochem Biophys Res Commun 354, 315–320

Weinstein H, Mehler EL (1994) $Ca^{2+}$-binding and structural dynamics in the functions of calmodulin. Annu Rev Physiol 56, 213–236

Westbroek P, Young JR, Linschooten K (1989) Coccolith production (biomineralization) in the marine algae *Emiliania huxleyi*. J Protozool 36, 368–373

Winter A, Jordan RW, Roth PH (1994) Biogeography of living coccolithophores in ocean waters. In: *Coccolithophores*, Winter A, Siesser WG (eds) Cambridge University Press, Cambridge, UK, pp. 161–177

Xu Y, Wahlund TM, Feng L, Shaked Y, Morel FMM (2006) A novel alkaline

phosphatase in the coccolithophore *Emiliania huxleyi* (Prymnesiophyceae) and its regulation by phosphorus. J Phycol 42, 835–844

Yoshimura T, Nishioka J, Saito H, Takeda S, Tsuda A, Wells ML (2007) Distributions of particulate and dissolved organic and inorganic phosphorus in North Pacific surface waters. Mar Chem 103, 112–121

Young JR, Didymus JM, Bown PR, Prins B, Mann S (1992) Crystal assembly and phylogenetic evolution in heterococcoliths. Nature 356, 516–518

Young JR, Davis SA, Bown PR, Mann S (1999) Coccolith ultrastructure and biomineralisation. J Struct Biol 126, 195–215

Zhang XB, Wang Y, Li H, Zhang WQ, Wu D, Mi HF (2004) The mouse FKBP23 binds to BiP in ER and the binding of C-terminal domain is interrelated with $Ca^{2+}$ concentration. FEBS Let 559, 57–60

Zondervan I (2007) The effects of light, macronutrients, trace metals and $CO_2$ on the production of calcium carbonate and organic carbon in coccolithophores – A review. Deep-Sea Res Part II 54, 521–537

Tables

**Table II-1.** Determined N-terminal amino acid sequence of the protein.

| Amino acid sequence |
| --- |
| AVTELKVEVYDGP |

**Table II-2.** Sequences found to produce significant alignments with determined N-terminal amino acid.

(A), Sequences found by EST database search. (B), Sequences found by *E. huxleyi* CCMP1516 genome database search.

A

| Sequences |
| --- |
| gb\|CX775415.1\| |
| gb\|GE165605.1\| |
| gb\|GE153280.1\| |
| gb\|GE164597.1\| |

B

| Sequences |
| --- |
| jgi\|Emihu1\|427610\|estExtDG_Genewise1Plus.C_460101 |
| jgi\|Emihu1\|445326\|estExtDG_fgenesh_newKGs_kg.C_4300007 |

Figures

**Figure I-1.** Time courses of $^{45}$Ca-incorporation into the coccoliths on the cell surface and in the cytosolic space of *Emiliania huxleyi*.

(A), $^{45}$Ca-incorporation into coccoliths (closed circles) and protoplasts (open circles). (B), Ratio of $^{45}$Ca incorporation into coccoliths *vs*. whole cells. Temperature for cell growth and the experiment was 20ºC.

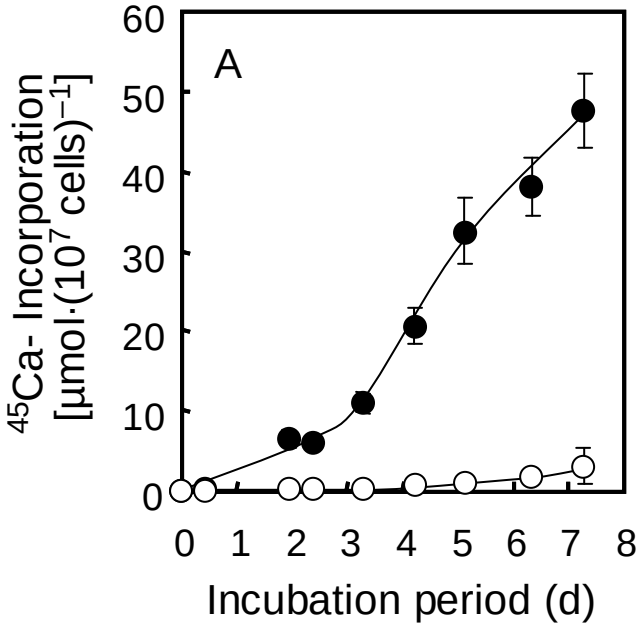
A
$^{45}$Ca- Incorporation
[µmol·(10$^{7}$ cells)$^{-1}$]
60
50
40
30
20
10
0
0 1 2 3 4 5 6 7 8
Incubation period (d)

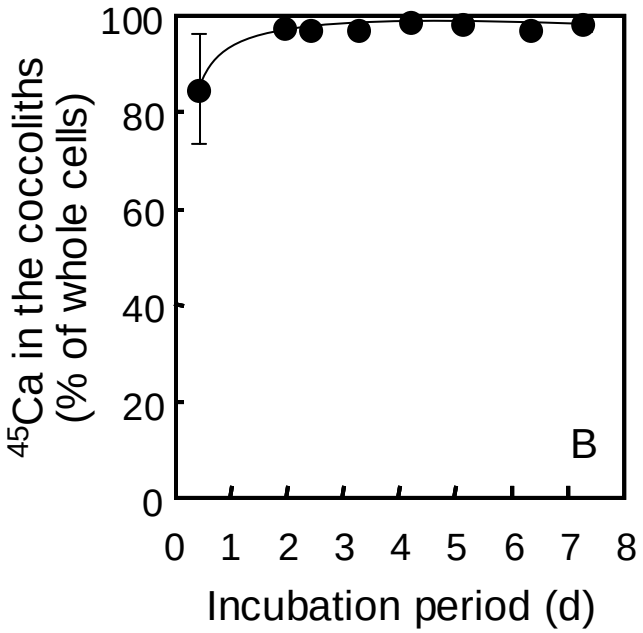
B
$^{45}$Ca in the coccoliths
(% of whole cells)
100
80
60
40
20
0
0 1 2 3 4 5 6 7 8
Incubation period (d)

**Figure I-2.** Changes in inorganic phosphate concentration, alkaline phosphatase activity, and calcification during growth of *Emiliania huxleyi*.

The cells were grown at 20ºC and then half of the culture was transferred to 12ºC (open symbols) while the remainder was maintained at 20ºC as a control (closed symbols) at 0 h (vertical line). (A), Cell numbers (circles) and inorganic phosphate concentration in the medium (squares). (B), Alkaline phosphatase (AP) activity. (C), $^{45}Ca$ incorporation into whole cells.

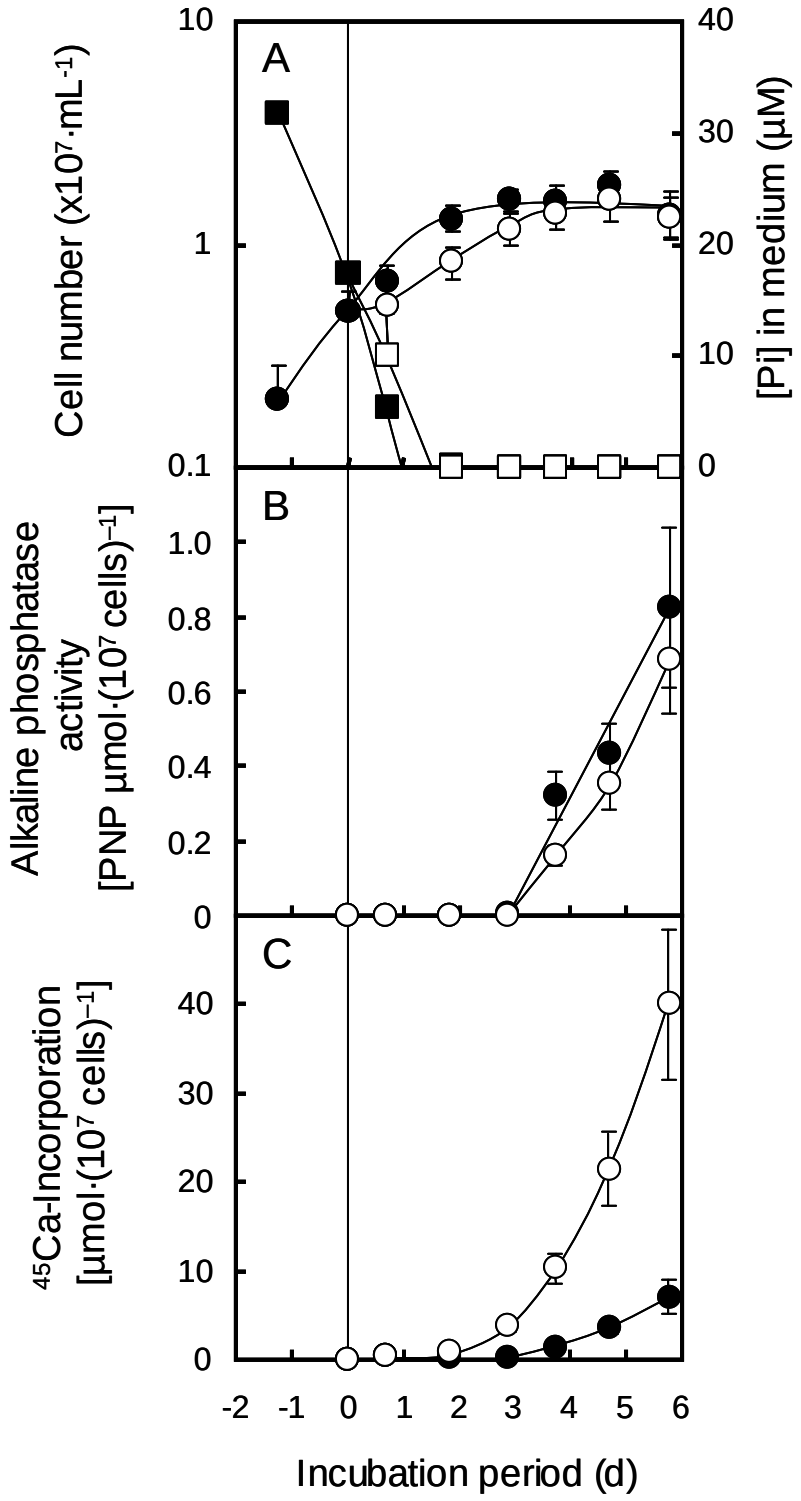
A
B
C
Cell number (x10⁷·mL⁻¹)
[Pi] in medium (µM)
Alkaline phosphatase activity [PNP µmol·(10⁷ cells)⁻¹]
⁴⁵Ca-Incorporation [µmol·(10⁷ cells)⁻¹]
Incubation period (d)
10
1
0.1
40
30
20
10
0
1.0
0.8
0.6
0.4
0.2
0
-2
-1
0
1
2
3
4
5
6

**Figure I-3.** Effect of phosphate on alkaline phosphatase activity and calcification in *Emiliania huxleyi*.

(A), Cells pre-grown in Pi-sufficient culture at 20ºC were transferred to Pi-sufficient (closed circles) and -deficient (open circles) conditions at time 0. (B), Dibasic potassium phosphate solution was added (arrow, final concentration, 27.8 μM) to cells grown in Pi-deficient medium for 2.8 d. In both A and B: a, Cell number. b, Alkaline phosphatase (AP) activity. c, $^{45}Ca$ incorporation into whole cells.

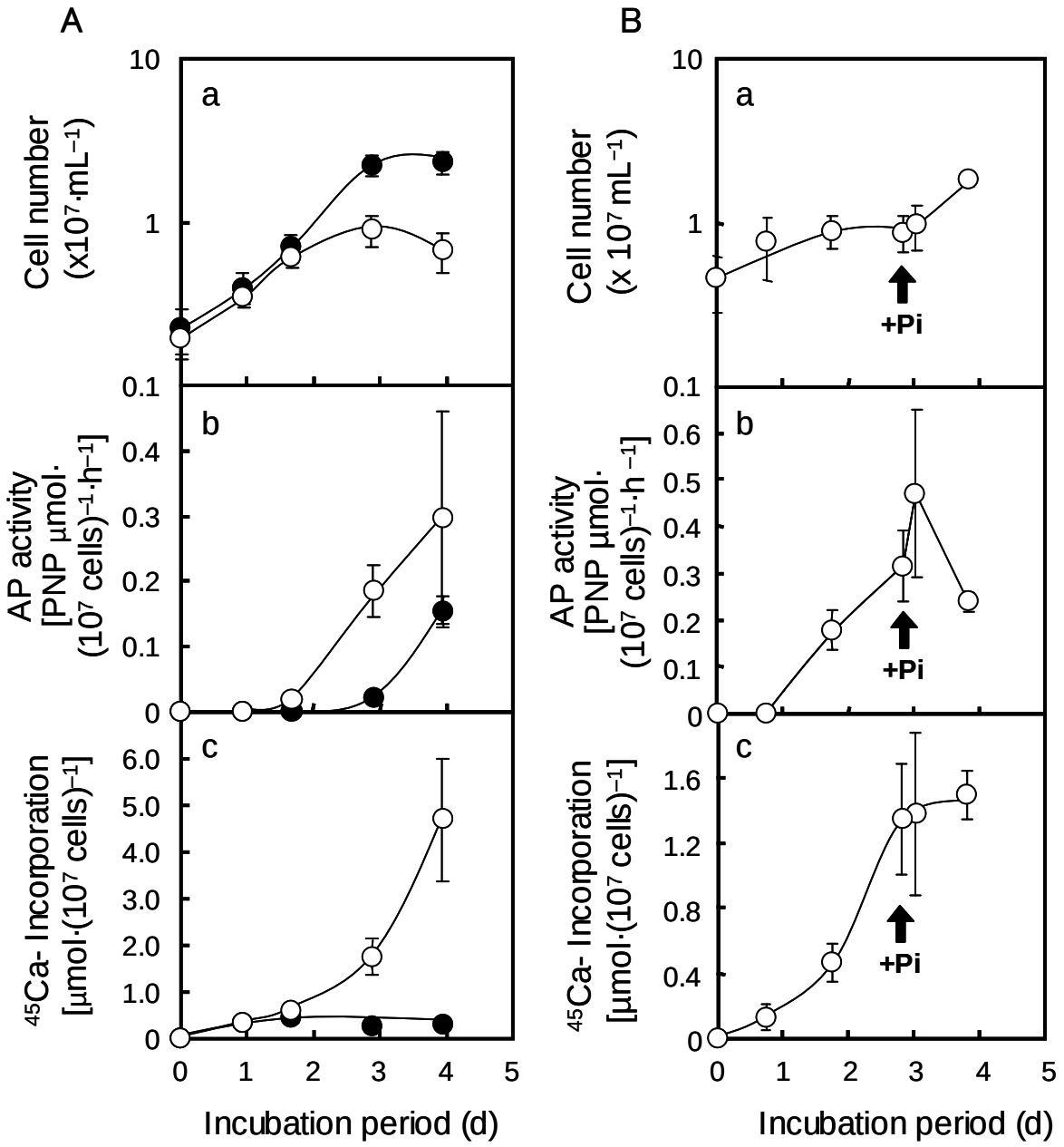
A
B
a
b
c
Cell number
(x10⁷·mL⁻¹)
Cell number
(x 10⁷ mL⁻¹)
AP activity
[PNP µmol·
(10⁷ cells)⁻¹·h⁻¹]
⁴⁵Ca- Incorporation
[µmol·(10⁷ cells)⁻¹]
+Pi
Incubation period (d)
Incubation period (d)

**Figure I-4.** Combined effect of phosphate deprivation and cold stress on calcification by *Emiliania huxleyi*.

The cells were grown at 20ºC and then transferred to 12ºC under Pi-sufficient (closed symbols) or -deficient (open symbols) conditions at 0 h (vertical line). For Pi-sufficient culture, the phosphate concentration was maintained above 20 μM by the addition of dibasic potassium phosphate solution (arrows). For Pi-deficient culture, phosphate concentration in the medium was rapidly decreased. (A), Changes in cell number (circles) and inorganic phosphate concentration in the medium (squares). (B), Alkaline phosphatase (AP) activity. (C), $^{45}$Ca incorporation into cells.

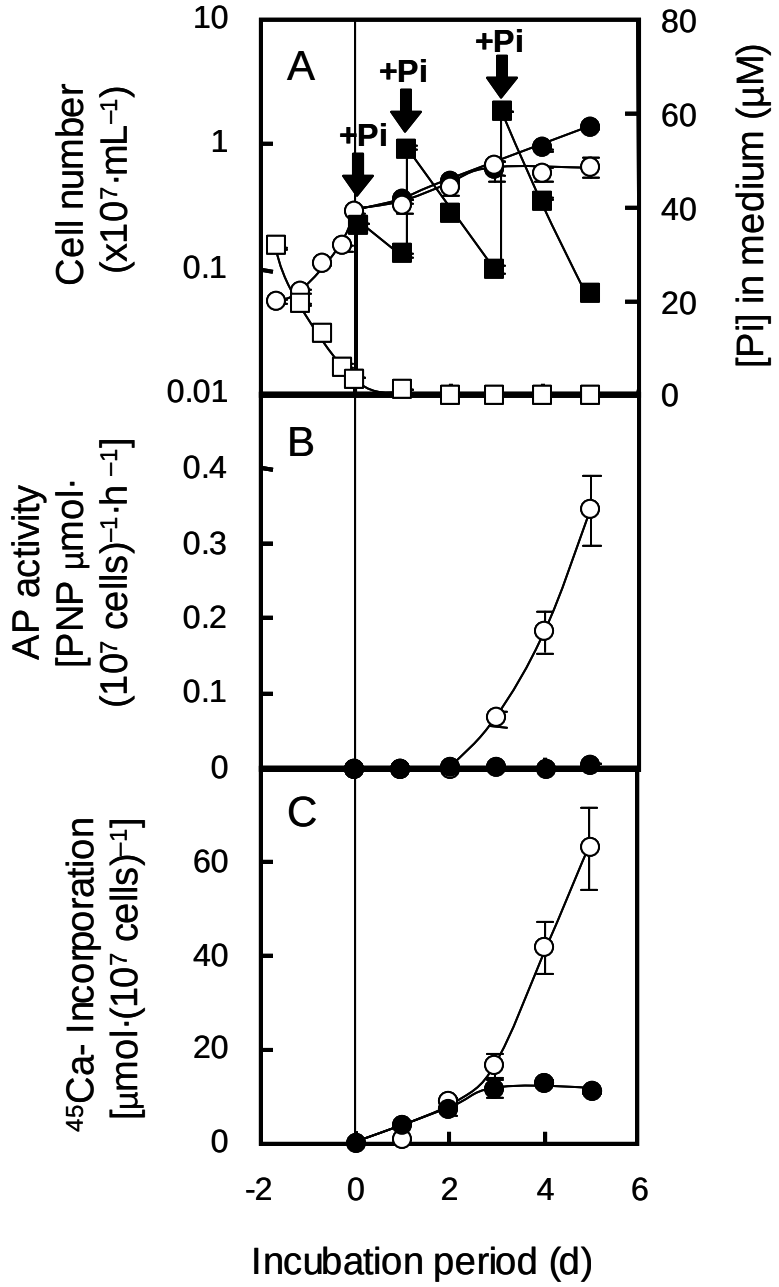
A
B
C
+Pi
+Pi
+Pi
Cell number
(x10⁷·mL⁻¹)
[Pi] in medium (µM)
AP activity
[PNP µmol·
(10⁷ cells)⁻¹·h⁻¹]
⁴⁵Ca- Incorporation
[µmol·(10⁷ cells)⁻¹]
Incubation period (d)
10
1
0.1
0.01
80
60
40
20
0
0.4
0.3
0.2
0.1
0
60
40
20
0
-2
0
2
4
6

**Figure I-5.** Microscopic observations of *Emiliania huxleyi* cells grown at 20ºC and 13ºC under phosphate-sufficient and -deficient conditions.

Cells in logarithmic growth at 20ºC were transferred to 13ºC under Pi-sufficient and -deficient conditions at 0 h (vertical line). Inorganic phosphate concentration in the medium was quantified every day and dibasic potassium phosphate solution was added periodically to maintain Pi-sufficient conditions. A portion of the culture was maintained at 20ºC as a control. (A), Changes in cell number. Closed circles, 20ºC without a supply of phosphate (control); Open circles, 13ºC without a supply of phosphate; Open triangles, 13ºC with supply of phosphate. (B), Photographs taken under bright-field microscopy (left) and polarization microscopy (right). a, Cells in logarithmic growth (time 0); b and c, Cells grown at 20ºC and 13ºC for 4 d without a supply of phosphate (Pi-deprived conditions), respectively; d, Cells grown at 13ºC for 4 d with a supply of phosphate (Pi-sufficient conditions). Magnification of photographs is the same in a–d. Scale bar, 5 µm.

A

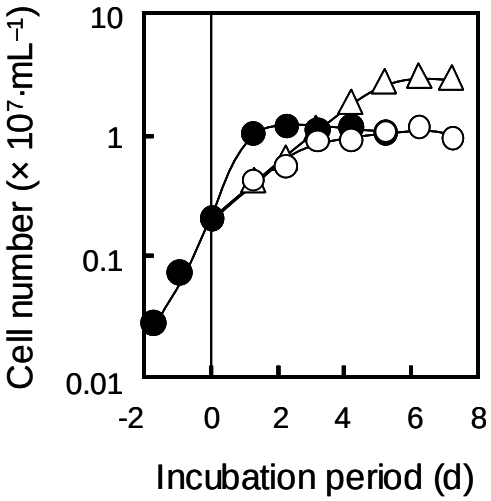
Cell number (× 10⁷·mL⁻¹)
10
1
0.1
0.01
-2
0
2
4
6
8
Incubation period (d)

B

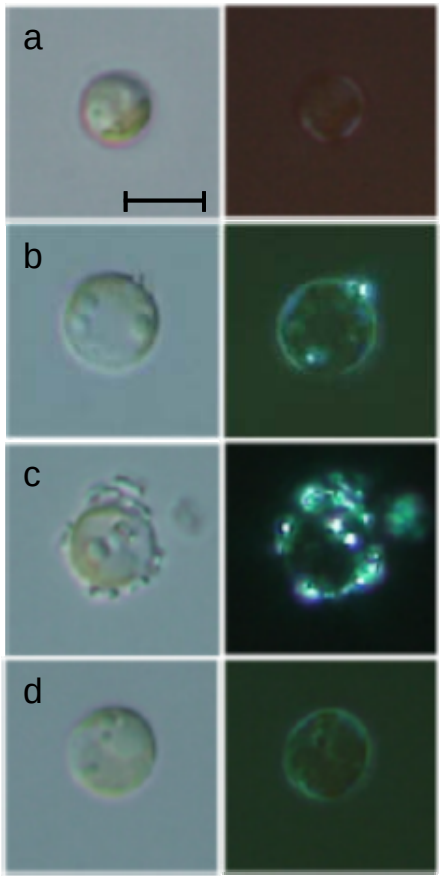
a
b
c
d

**Figure II-1.** Schematic representation of *Emiliania* cells showing three stages (1-3) of coccolith formation. Upper cell also shows extracellular coccoliths. (Modified from de Vrind-de Jong and de Vrind, 1997)

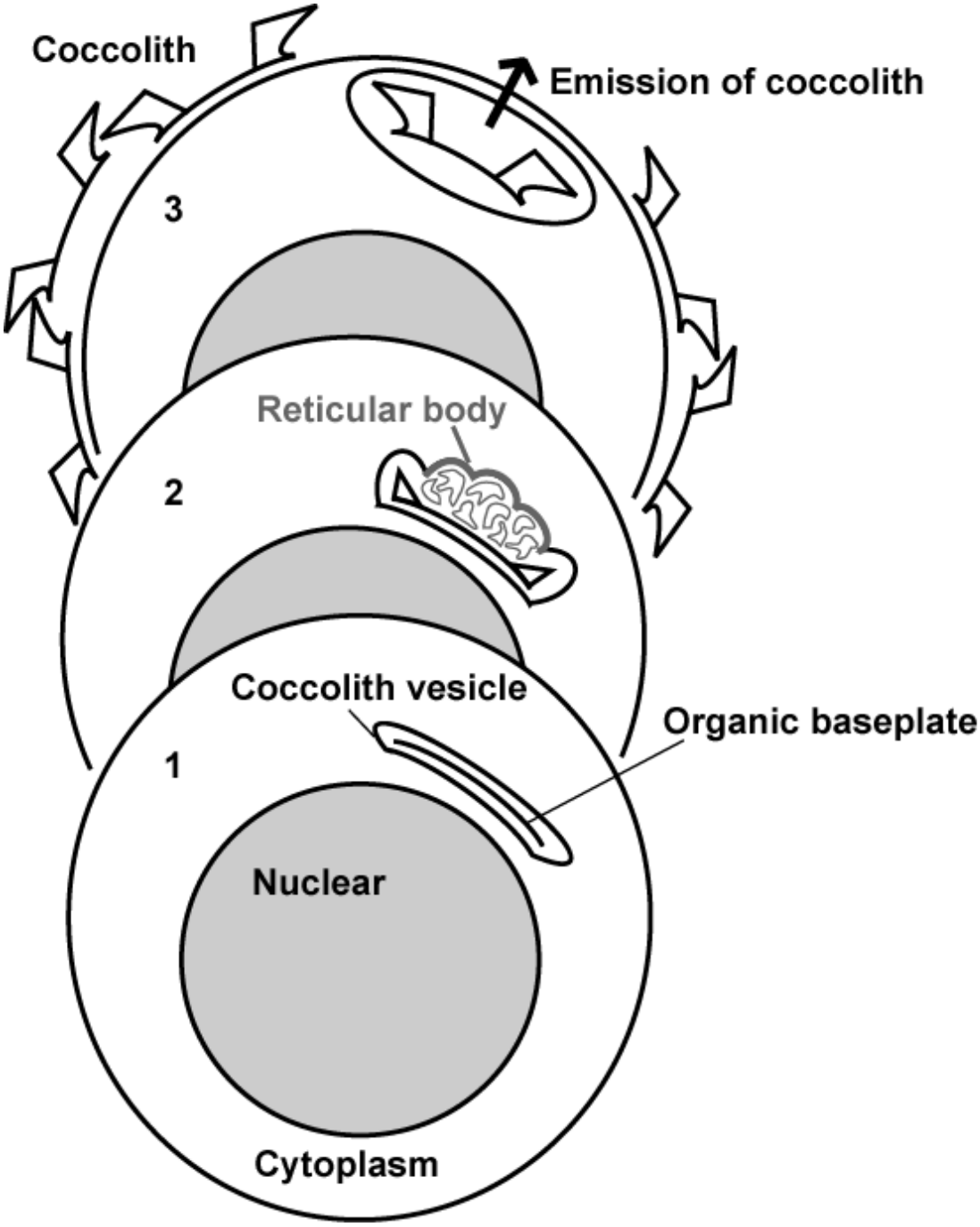
Coccolith
Emission of coccolith
3
Reticular body
2
Coccolith vesicle
Organic baseplate
1
Nuclear
Cytoplasm

**Figure II-2.** Monitoring of calcification by $^{45}$Ca-incorporation and the analysis of $^{35}$S-labeled proteins.

*E. huxleyi* cells grown at 20°C in the bubbling culture for 3.9 d were transferred to either Pi-sufficient or -deficient conditions at time 0. (A), Time course of $^{45}$Ca incorporation into cells. Closed and open circles, Pi-sufficient and Pi-deficient conditions, respectively. (B), Radioluminographs of SDS-PAGE profiles of $^{35}$S-labeled proteins synthesized *de novo*. Metabolic labeling of proteins with $^{35}$S was performed by incubating cells with $^{35}$S-Met/Cys for 1 h from 96 h to 97 h in culture. Lanes 1 and 2, cells grown under Pi-sufficient and -deficient conditions, respectively. The migration of molecular mass markers is shown on the left. Arrowheads indicate the proteins of which the synthesis increased under Pi-deficient conditions where the calcification was stimulated as shown in Fig. II-2A.

A

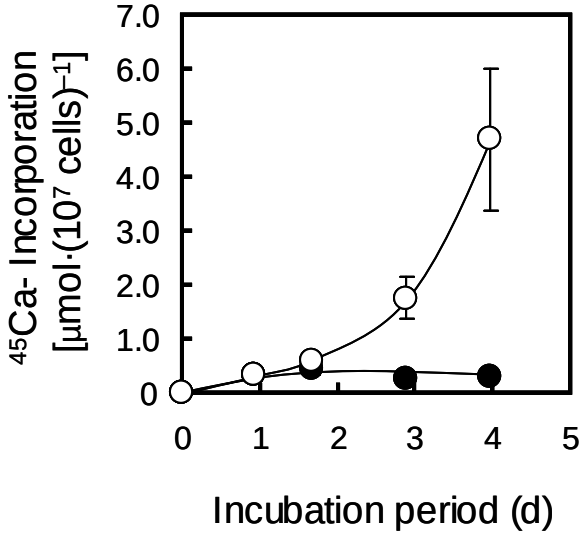
7.0
6.0
5.0
4.0
3.0
2.0
1.0
0
45Ca- Incorporation
[µmol·(10^7 cells)^-1]
0
1
2
3
4
5
Incubation period (d)

B

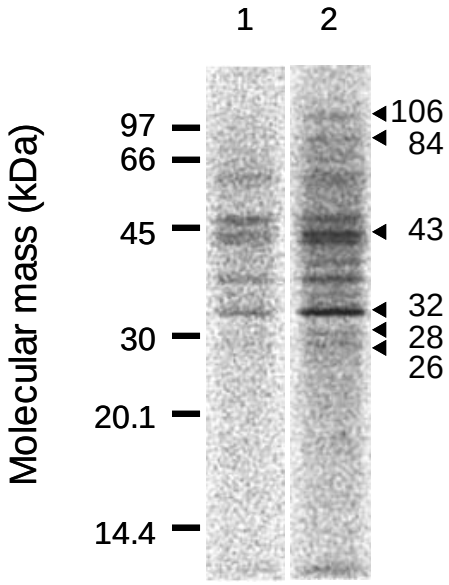
1
2
Molecular mass (kDa)
97
66
45
30
20.1
14.4
106
84
43
32
28
26

**Figure II-3.** Effect of Pi on $^{45}$Ca incorporation into cells, a parameter of calcification, and SDS-PAGE profiles of $^{35}$S-labeled proteins in cells grown under phosphate-deficient and -sufficient conditions.

*E. huxleyi* cells grown at 20°C for 2.9 d were transferred to Pi-deficient conditions at time 0. After 2.9 d incubation, dibasic potassium phosphate solution (final concentration, 27.8 μM) was added. (A), Effect of Pi on $^{45}$Ca incorporation into cells. (B), SDS-PAGE analysis of the *de novo* synthesized $^{35}$S-labeled proteins by using radioluminography. First, cells were grown in Pi-free medium for 69 h. Metabolic $^{35}$S-labeling of the protein by $^{35}$S-Cys/Met was performed in the absence and presence of Pi. Lane 1, Pi-deficient cells. Lane 2, Pi-sufficient cells. Arrowheads, proteins in which the $^{35}$S-labeling amount increased under Pi-deficient, and decreased under Pi-sufficient condition.

A

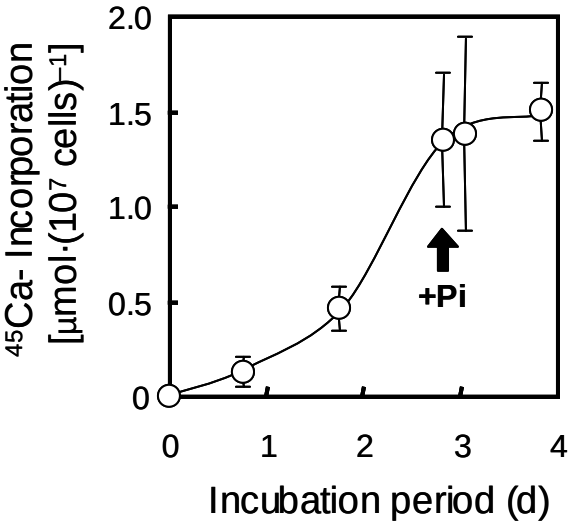
2.0
1.5
1.0
0.5
0
$^{45}$Ca- Incorporation
[µmol·(10$^7$ cells)$^{-1}$]
+Pi
0
1
2
3
4
Incubation period (d)

B

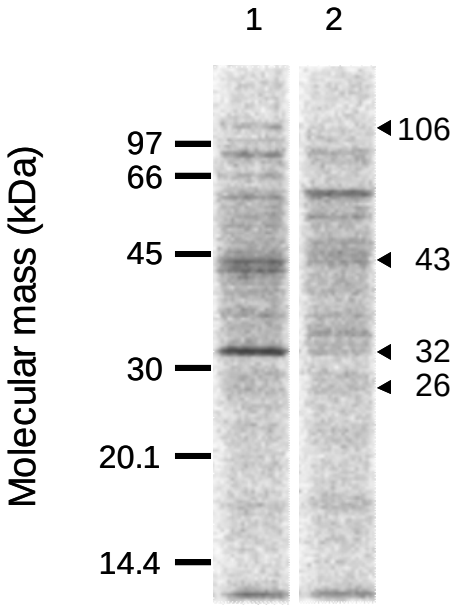
1
2
Molecular mass (kDa)
97
66
45
30
20.1
14.4
106
43
32
26

**Figure II-4.** Effect of temperature change on $^{45}$Ca incorporation into cells, a parameter of calcification, and SDS-PAGE profiles of $^{35}$S-labeled proteins in cells grown at 12ºC and 20ºC.

The cells grown at 20ºC for 1.3 d in the basal medium were divided into two. And then each culture was transferred to either 12ºC (cold stress) or 20ºC (control). (A), $^{45}$Ca incorporation into whole cells. Closed circles, 20°C. Open circles, 12°C. (B), SDS-PAGE analysis of the *de novo* synthesized $^{35}$S-labeled proteins by using radioluminography. Metabolic $^{35}$S-labeling of the protein by $^{35}$S-Cys/Met was performed for 1 h. Lane 1, 12°C, 44.5–45.5 h. Lane 2, 20°C, 139–140 h. Lane 3, 12°C, 139–140 h. Arrowhead, 32-kDa protein.

A

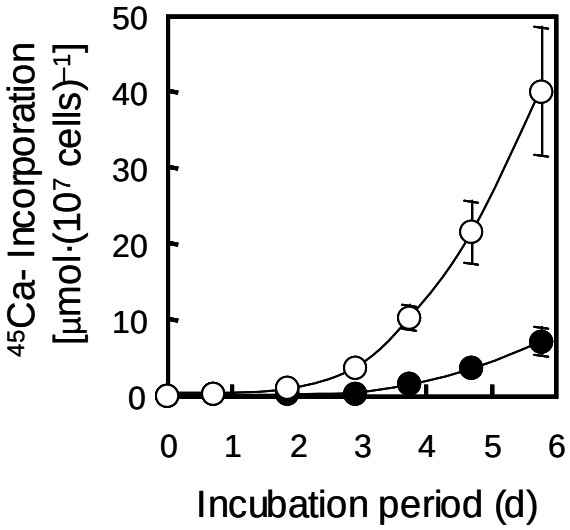
$^{45}$Ca- Incorporation
[µmol·(10$^7$ cells)$^{-1}$]
50
40
30
20
10
0
0 1 2 3 4 5 6
Incubation period (d)

B

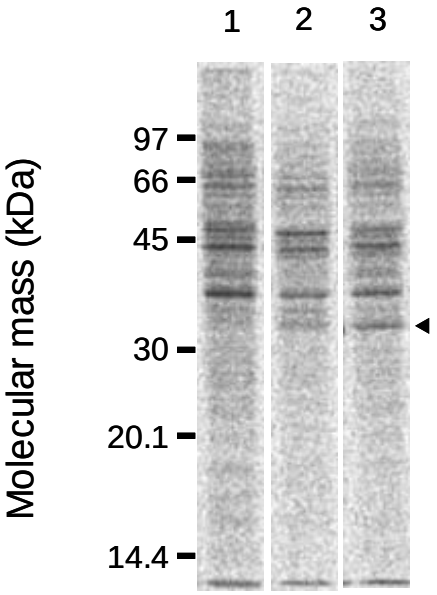
1 2 3
Molecular mass (kDa)
97
66
45
30
20.1
14.4

**Figure II-5.** Purification of a 32-kDa protein assumed to be associated with coccolith production.

Cells were incubated at 12°C for 5 d and then labeled with $^{35}$S-Cys/Met. Proteins were extracted with 50 mM Tris-HCl (pH 7.0) and the soluble fraction was subjected to further purification. (A), Radioluminography profiles on SDS-PAGE of the fractionation of acetone precipitation. Lane 1, fraction obtained by 20–40% acetone-treatment. Lane 2, 40–75% acetone-treatment. Lane 3, 60% acetone-precipitation. Lane 4, 60–75% acetone-treatment. (B), Anion-exchange chromatography of 40–60% acetone-fraction. The dotted line, solid line and column represent $(NH_4)_2SO_4$ concentration, $A_{280}$ for proteins and radioactivity of $^{35}$S in the eluted fractions, respectively. (C), SDS-PAGE analysis of fraction #16 in Fig. II-5B. Ag and $^{35}$S, the silver staining and $^{35}$S-radioactive bands, respectively. Arrowheads in Fig. II-5A and C, 32-kDa protein.

A

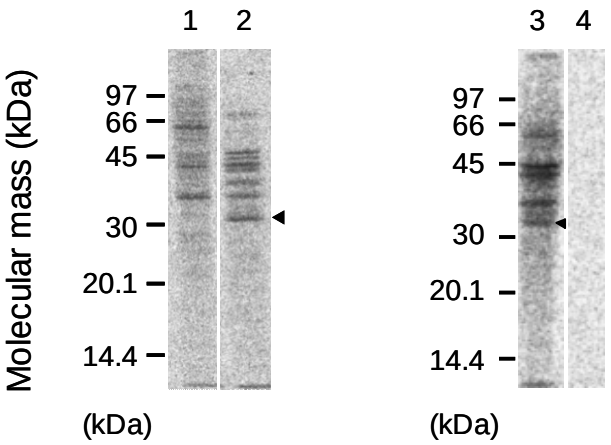
1 2
3 4
Molecular mass (kDa)
97
66
45
30
20.1
14.4
(kDa)
(kDa)

B

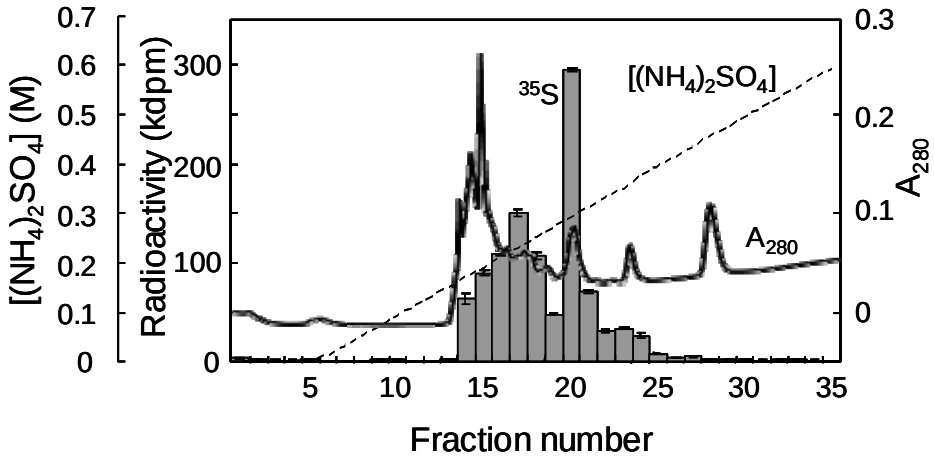
[(NH4)2SO4] (M)
Radioactivity (kdpm)
A280
35S
[(NH4)2SO4]
A280
Fraction number

C

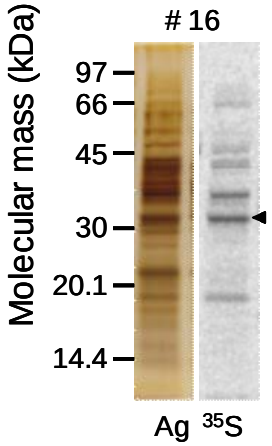
# 16
Molecular mass (kDa)
97
66
45
30
20.1
14.4
Ag 35S

**Figure II-6.** Comparison of IEF/SDS-PAGE patterns of $^{35}$S-labeled proteins extracted from cells grown between under Pi-deficient condition and at low temperature.

(A), Soluble fraction extracted from the phosphate deficient cells which were grown in Pi-free medium for 4 d. (B), Fraction #16 in Fig. II-5C that contains partially purified proteins from the cells grown at 12°C for 5d. (C), Mixture of samples in Fig.II-6A and B. Left and right, the silver stained and $^{35}$S radioactive gels, respectively. Boxes, SDS-PAGE profiles of the same samples applied to 2D-PAGE analyses. Arrowheads, 32-kDa protein.

A

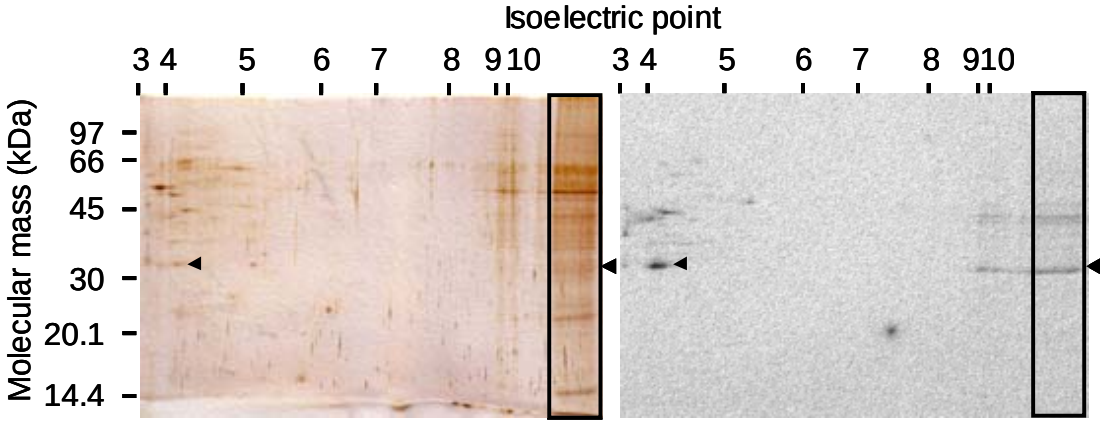
Isoelectric point
3 4 5 6 7 8 9 10
3 4 5 6 7 8 9 10
Molecular mass (kDa)
97
66
45
30
20.1
14.4

B

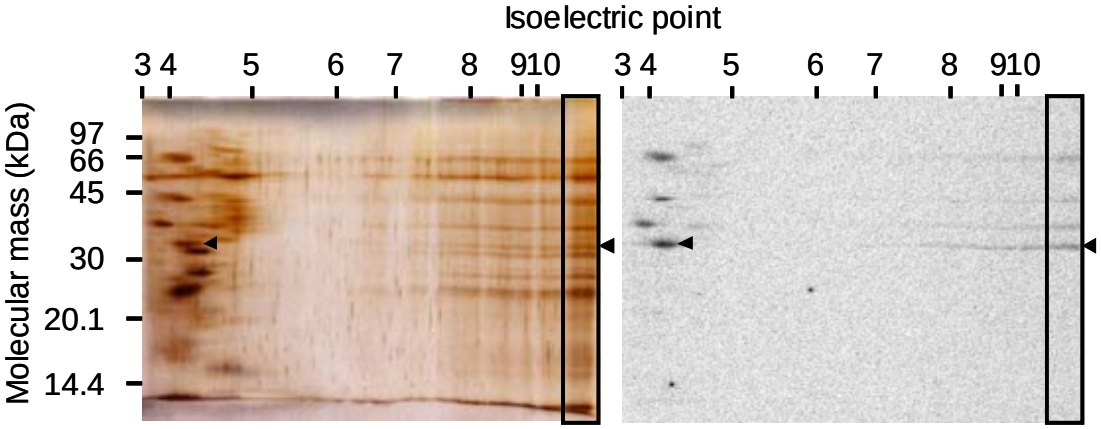
Isoelectric point
3 4 5 6 7 8 9 10
3 4 5 6 7 8 9 10
Molecular mass (kDa)
97
66
45
30
20.1
14.4

C

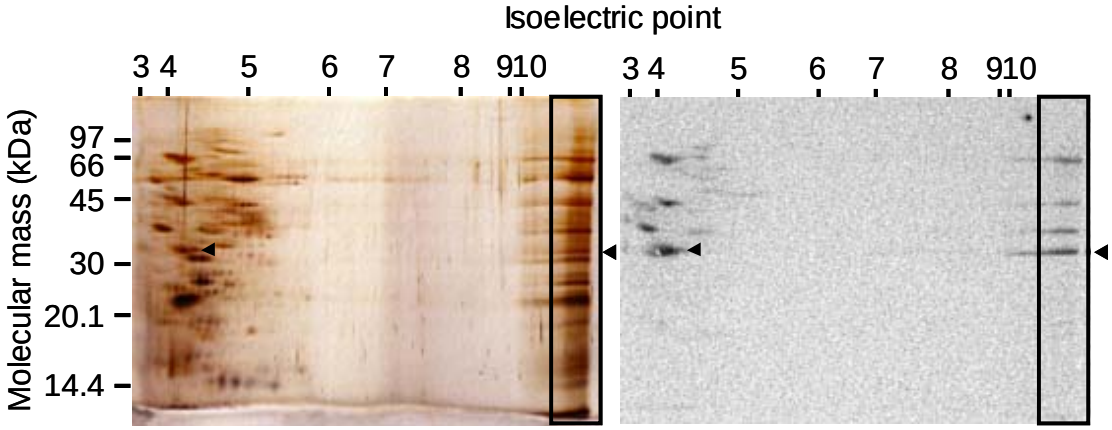
Isoelectric point
3 4 5 6 7 8 9 10
3 4 5 6 7 8 9 10
Molecular mass (kDa)
97
66
45
30
20.1
14.4

**Figure II-7.** Sequence analyses of the deduced amino acid sequence of EhFKBP21.

*Thin underline,* FKBP-type peptidyl-prolyl *cis-trans* isomerase domain; *asterisks,* two potential calcium binding sites of EF-hand motif; Lowercase, a putative signal peptide ; arrowhead, the most probable site of post-translational cleavage; highlighted boldface type, N-terminal amino acid sequence determined experimentally; *underlined* with *dots,* the endoplasmic reticulum retaining signal, C-terminal KDEL motif ; *bold underlines with α and β,* predicted second structure; α helix and consecutively numbered β strands.

```
>EhFKBP21

  1  mllacsllas gaaaAVTELK VEVYDGPKEC EDADKLKKGE
                     ▲        β-I
 41  HVSMHYTGTI DKDSAAGTPG KQFDSSRGRG KTFDFQLGAG
        β-II                β-III          β-IV
 81  RVIQGWDKGL EGLCVGAKAV LTIPPDMGYG ARGAGGDIPG
          α            β-V
121  GAALSFDVEV VSHSDEGPPE PNLFKDLDTD KDAKLTQEEV
        β-VI                         * *  *     *
161  LAFFKQQGKE ELPEGLWEKE DKDKDGFISW EEFGGPKGKS
                            * * *       *

201  KDEL
```

**Figure II-8.** Comparison of amino acid sequences among various FKBPs and the EF-hand $Ca^{2+}$ binding domains.

(A), Alignment of the amino acid sequence of the FKBP-type PPIase domain of EhFKBP21 with the FKBP-type PPIase domain of *Drosophila melanogaster* FKBP13 (DmFKBP13), mouse FKBP23 (mFKBP23), *Arabidopsis thaliana* FKBP15-2 (AtFKBP15-2), *Chlamydomonas reinhardtii* FKB15-2 (FKB15-2) and human FKBP12 (hFKBP12), and the Genbank™ accession numbers for the sequences were NP_726074, NP_034352, NP_199669, EDP00314 and NP_000792. DmFKBP13, mFKBP23, AtFKBP15-2 and FKB15-2 are predicted to locate in ER like EhFKBP21. Black arrowheads and dots denote FK506 binding site and hydrophobic pockets, respectively, according to van Duyne et al. (1991). (B), Alignment of the EF-hand $Ca^{2+}$ binding domain of calmodulin with mFKBP23 and EhFKBP21. Asterisks, sharp and dot indicate amino acids with oxygen containing side chain, consensus hydrophobic amino acids and highly conserved glycine, respectively. Identical amino acid residues are shown in black boxes; analogous amino acids are shaded.

A

```
AtFKBP15-2   52  GDTIKVHYRG KLT------- DGTVFDSSFE R--GDPFEFK
FKB15-2      53  GDWVGVHYVG KLE------- NGEEFDNSIT R--GEPIEFQ
mFKBP23      49  GDLLNAHYDG YLAK------ DGSKFYCSRT QDEGHPKWFV
DmFKBP13     59  GDSLTMHYTG TLQA------ DGKKFDSSFD R--DQPFTFQ
EhFKBP21     39  GEHVSMHYTG TIDKDSAAGT PGKQFDSSRG R--GKTFDFQ
hFKBP12          GQTCVVHYTG MLE------- DGKKFDSSRD R--NKPFKFM
                   •                       ▲                •
                 Tyr26                   Asp37            Phe46

AtFKBP15-2   83  LGSGQVIKGW DQGLLGACVG EKRKLKIPAK LGYGEQG-SP
FKB15-2      84  LGAQQVIAGW ETGILGMCVG EKRRLHIPPH LAYGDEG-A-
mFKBP23      83  LGVGHVIKGL DIAMMDMCPG EKRKVIIPPS FAYGKEGYAE
DmFKBP13     91  LGAGQVIKGW DQGLLNMCVG EKRKLTIPPQ LGYGDQG-AG
EhFKBP21     77  LGAGRVIQGW DKGLEGLCVG AKAVLTIPPD MGYGARG-AG
hFKBP12          LGKQEVIRGW EEGVAQMSVG QRAKLTISPD YAYGATG-HP
                   ••    •                                ▲
                ▲▲ ▲  Gln53 Glu54 Val55 Ile56 Trp59      Tyr82

AtFKBP15-2  122  PTIPGGATLI FDTELIAVN
FKB15-2     122  GPIPAGASLV FDVELVRIT
mFKBP23     123  GKIPPNATLM FEIELYAVT
DmFKBP13    130  NVIPPKATLL FDVELINIG
EhFKBP21    116  GDIPGGAALS FDVEVVSHS
hFKBP12          GIIPPHATLV FDVELLKLE
                              •
                            Phe99
```

B

```
                 Helix        Loop        Helix
I                FKEAFSLF  DKDGDGTITTKE  LGTVMRSL
II               LQDMINIV  DADGNGTIDFPE  FLTMMARK
III              IREAFRVF  DKDGNGYISAAE  LRHVMTNL
IV               VDEMIREA  DIDGDGQVNYEE  FVQMMTAR
mFKBP23_I        SIETFKQI  DTDNDRQLSKAE  IELYLQKD
mFKBP23_II       LEDIFKKN  DHNGDGFISPKE  YNVHQHDE
EhFKBP21_I       EPNLFKDL  DTDKDAKLTQEE  VLAFFKQQ
EhFKBP21_II      PEGLWEKE  DKDKDGFISWEE  FGGPKGKS
                            *  *  *•  #*   *
```

**Figure II-9.** Effect of FK506 on the growth and the calcification of *Emiliania huxleyi*.

Cells grown in Pi-sufficient culture at 20ºC were transferred to Pi-deficient conditions at time 0 and FK506 (final concentration, 1μM) was added after 1.9 d incubation. Open circles and closed circles, in the absence and presence of FK506, respectively. (A), Changes in cell number. (B), $^{45}Ca$ incorporation by cells containing in 1 mL suspension. (C), $^{45}Ca$ incorporation into cells.

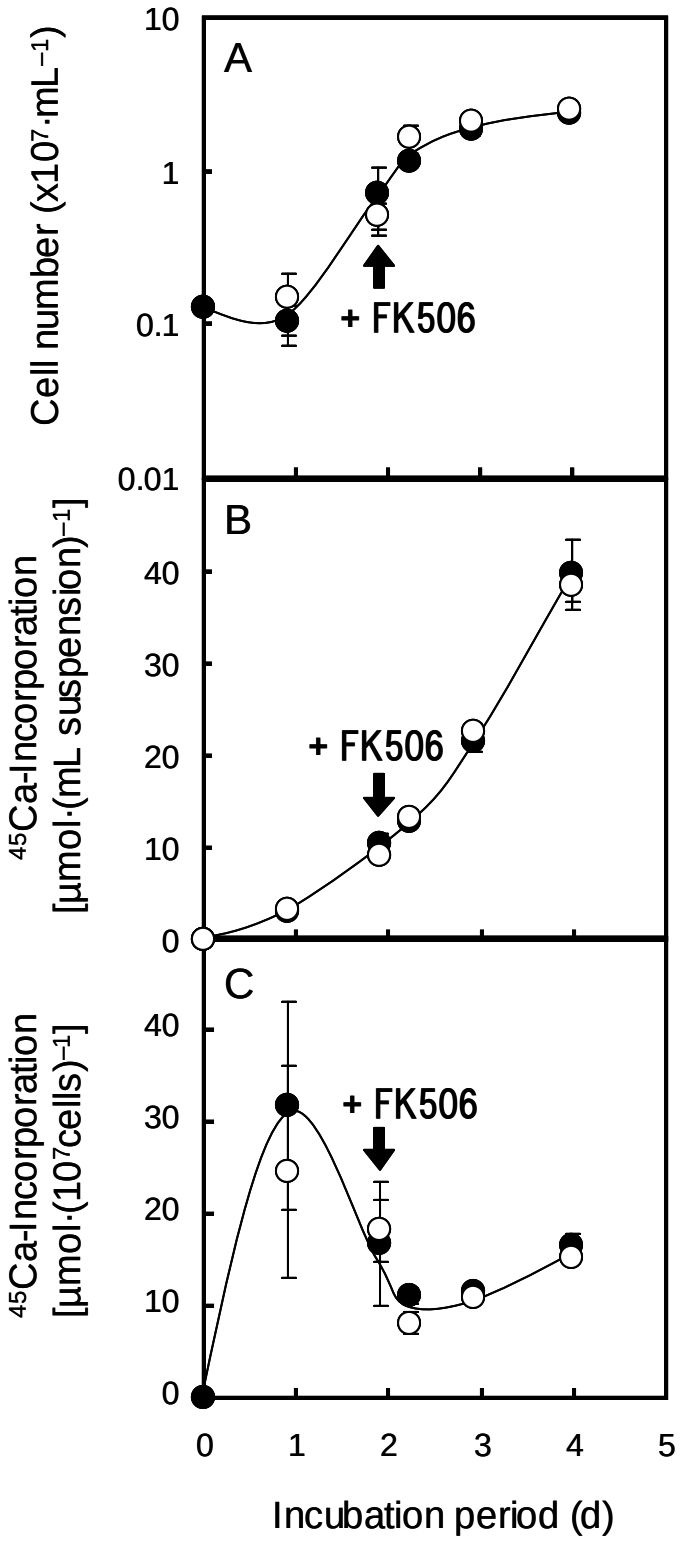
A
B
C
Cell number (x10⁷·mL⁻¹)
45Ca-Incorporation [µmol·(mL suspension)⁻¹]
45Ca-Incorporation [µmol·(10⁷cells)⁻¹]
+ FK506
+ FK506
+ FK506
10
1
0.1
0.01
40
30
20
10
0
0
1
2
3
4
5
Incubation period (d)

Acknowledgments

I would like to express my sincerest gratitude to my supervisor Prof. Yoshihiro Shiraiwa for his generous consultation and continuous encouragement. I appreciate Associate Prof. Iwane Suzuki for his critical discussion. I am also thankful to Dr. Koji Iwamoto for his support and valuable discussion. I thank Prof. Isao Inouye and his laboratory members of the University of Tsukuba for their kind support in microscopic observations. I also thank the staffs of the Radioisotope Center of the University of Tsukuba, for their kind help with the radioisotope experiments. This work was supported in part by the Sasakawa Scientific Research Grant from the Japan Science Society (15-365M, that was funded to me in 2003).